© 2014. Published by The Company of Biologists Ltd | Journal of Cell Science (2014) 127, 2601 doi:10.1242/jcs.154898

CORRECTION

PI4KIIIα is required for cortical integrity and cell polarity during *Drosophila* oogenesis

Julie Tan, Karen Oh, Jason Burgess, David R. Hipfner and Julie A. Brill

There was an error published in *J. Cell Sci.* **127**, 954-966.

The synonym for $l(1)3Ah^{21}$ was incorrectly identified as $zw2^{c21}$ on pages 955 and 963 of this article. The correct synonym is $zw2^{123}$, not to be confused with the allele generated in this study, which is $PI4KIII\alpha^{\Delta 123}$.

Accordingly, on page 955, the sentence 'Like $PI4KIII\alpha^{\Delta 123}$, males hemizygous for $zw2^{c21}$ or other *zw2* alleles die as first instar larvae (Shannon et al., 1972).' should read 'Like $PI4KIII\alpha^{\Delta 123}$, males hemizygous for other *zw2* alleles die as first instar larvae (Shannon et al., 1972).'

The authors apologise to the readers for any confusion that this error might have caused.

© 2014. Published by The Company of Biologists Ltd | Journal of Cell Science (2014) 127, 954–966 doi:10.1242/jcs.129031

RESEARCH ARTICLE

PI4KIIIα is required for cortical integrity and cell polarity during *Drosophila* oogenesis

Julie Tan[1,2], Karen Oh[3], Jason Burgess[1,2], David R. Hipfner[3,4] and Julie A. Brill[1,2,*]

ABSTRACT

Phosphoinositides regulate myriad cellular processes, acting as potent signaling molecules in conserved signaling pathways and as organelle gatekeepers that recruit effector proteins to membranes. Phosphoinositide-generating enzymes have been studied extensively in yeast and cultured cells, yet their roles in animal development are not well understood. Here, we analyze *Drosophila melanogaster* phosphatidylinositol 4-kinase IIIα (PI4KIIIα) during oogenesis. We demonstrate that PI4KIIIα is required for production of plasma membrane PtdIns4*P* and PtdIns(4,5)P_2 and is crucial for actin organization, membrane trafficking and cell polarity. Female germ cells mutant for *PI4KIIIα* exhibit defects in cortical integrity associated with failure to recruit the cytoskeletal-membrane crosslinker Moesin and the exocyst subunit Sec5. These effects reflect a unique requirement for PI4KIIIα, as egg chambers from flies mutant for either of the other *Drosophila* PI4Ks, *fwd* or *PI4KII*, show Golgi but not plasma membrane phenotypes. Thus, PI4KIIIα is a vital regulator of a functionally distinct pool of PtdIns4*P* that is essential for PtdIns(4,5)P_2-dependent processes in *Drosophila* development.

KEY WORDS: PI 4-kinase, Phosphatidylinositol 4-phosphate, PI4*P*, PI(4,5)P_2, Exocyst, Moesin

INTRODUCTION

Although phosphoinositides constitute only a small percentage of membrane lipids, they exert powerful effects on many cellular processes. The seven phosphoinositide species are named according to the combination of phosphate groups present on the 3-, 4- and 5-positions of the inositol ring. Phosphatidylinositol 4-kinases (PI4Ks) catalyze conversion of phosphatidylinositol (PtdIns) to phosphatidylinositol 4-phosphate (PtdIns4*P*), the first step in generating the majority of phosphoinositides in the cell. PtdIns4*P* itself has emerged as a key regulator of membrane trafficking at the Golgi because of its binding to and recruitment of effectors such as clathrin adaptors, coat proteins and lipid transfer proteins (D'Angelo et al., 2012). Interestingly, despite the importance of PtdIns4*P* in intracellular membrane compartments, it has been suggested that the majority of PtdIns4*P* resides at the plasma membrane (PM) (Hammond et al., 2009).

[1]Program in Cell Biology, The Hospital for Sick Children, PGCRL, 686 Bay Street, Room 15.9716, Toronto, ON, M5G 0A4, Canada. [2]Department of Molecular Genetics, University of Toronto, 1 King's College Circle, Toronto, ON, M5S 1A8, Canada. [3]Epithelial Cell Biology, Institut de Recherches Cliniques de Montreal, 110, Avenue des Pins Ouest, Montreal, Quebec, H2W 1R7, Canada. [4]Department of Medicine, University of Montreal, Montreal, QC, H3T 3J7, Canada.

*Author for correspondence (julie.brill@sickkids.ca)

Received 8 February 2013; Accepted 2 December 2013

PtdIns4*P* is the metabolic precursor of phosphatidylinositol 4,5-bisphosphate [PtdIns(4,5)P_2], which mainly resides at the PM, where it regulates diverse processes such as cytokinesis, cell migration, cell polarization, cell adhesion and cell morphogenesis (Brill et al., 2011; Echard, 2012; Saarikangas et al., 2010; Shewan et al., 2011; Zhang et al., 2012). Some of these processes are governed by second messengers that are formed by phospholipase C (PLC)-dependent hydrolysis of PtdIns(4,5)P_2. Others are accomplished by recruitment of effector proteins that specifically bind PtdIns(4,5)P_2. For example, PtdIns(4,5)P_2 recruits AP-2 and dynamin during endocytosis and the exocyst complex during exocytosis (Gaidarov and Keen, 1999; Martin, 2012; Vallis et al., 1999). In flies and in mammalian cells, PtdIns(4,5)P_2 localizes the exocyst to sites of polarized exocytosis, presumably by binding directly to the polybasic domains of the Sec3 and Exo70 subunits, as was shown in yeast (Fabian et al., 2010; He et al., 2007; Thapa et al., 2012; Xiong et al., 2012). Furthermore, PtdIns(4,5)P_2 recruits and activates actin regulators, including the cytoskeletal–PM crosslinker Moesin, which requires PtdIns(4,5)P_2-binding and subsequent phosphorylation to relieve autoinhibited occlusion of its F-actin-binding site (Fievet et al., 2004). The crucial role of PtdIns(4,5)P_2 at the PM lends interest to recent evidence showing that its precursor, PtdIns4*P*, has independent dynamics from PtdIns(4,5)P_2 and suggesting that PtdIns4*P* itself can play a role in defining PM identity (Hammond et al., 2012). Although *in vitro* functional studies are beginning to emerge, few experiments have addressed the role of PM PtdIns4*P* and the extent to which it is tied to PtdIns(4,5)P_2 during animal development.

Much of what we know about PtdIns4*P* has been elucidated through studying PI4Ks. These enzymes fall into two classes: type III PI4Ks, which share biochemical properties with the PI3K family of enzymes, and type II PI4Ks, which are unrelated (Balla and Balla, 2006). PI4KIIIα and PI4KIIβ exert their functions at the PM, whereas PI4KIIIβ and PI4KIIα affect Golgi and endosomes. Budding yeast has three PI4Ks, STT4 (PI4KIIIα), PIK1 (PI4KIIIβ) and LSB6 (PI4KII). STT4 and PIK1 have non-overlapping essential roles (Audhya and Emr, 2002; Audhya et al., 2000), whereas LS6B is dispensable (Han et al., 2002). STT4 localizes at the PM, where it regulates actin organization, vacuole morphology and PKC1–MAPK signaling. In contrast, PIK1 has essential functions in the nucleus and at the Golgi, where it directs secretion (Strahl et al., 2005). These disparate functions of yeast PI4Ks are roughly paralleled in mammalian cells, where PI4KIIIα controls a hormone-sensitive pool of PtdIns4*P* at the PM and PI4KIIIβ and PI4KIIα control Golgi PtdIns4*P* and post-Golgi trafficking (Balla et al., 2005; Jović et al., 2012; Weixel et al., 2005).

PI4Ks are crucial for cell homeostasis, yet only a handful of studies address their functions in multicellular organisms (Brill et al., 2000; Burgess et al., 2012; Khuong et al., 2010; Ma et al.,

Journal of Cell Science

Journal of Cell Science (2014) 127, 954–966 doi:10.1242/jcs.129031

2009; Polevoy et al., 2009; Raghu et al., 2009; Simons et al., 2009; Yan et al., 2011; Yavari et al., 2010). A recent report examining mouse PI4KIIIα revealed transient localization of PI4KIIIα to the PM (Nakatsu et al., 2012). However, because *PI4KIIIα* (also known as *Pi4Ka*) is essential, it was possible to examine genetic nulls only in primary cultures of induced knockout embryonic fibroblasts (MEFs). Hence, the role of PI4KIIIα during animal development has remained a mystery.

The fruit fly *Drosophila melanogaster* provides a tractable system to examine cellular roles of essential genes; using genetic tools that are more cumbersome to generate in mammals, it is possible to analyze mutant tissues in otherwise normal flies. *Drosophila* has three PI4Ks. We previously showed that the PIK1 and LSB6 homologues Four wheel drive (Fwd) and PI4KII play roles in post-Golgi trafficking, but are not essential (Brill et al., 2000; Burgess et al., 2012). Fwd localizes to the Golgi where it is needed for spermatocyte cytokinesis (Polevoy et al., 2009), whereas PI4KII localizes to Golgi and endosomes and is required for secretory granule biogenesis in the larval salivary gland (Burgess et al., 2012). Here, we examine the requirement for PI4KIIIα, which we show is essential and needed for structural integrity of the PM during oogenesis. PI4KIIIα is required for activation and recruitment of Moesin and Sec5, effector proteins that organize the cell cortex. These roles are specific to PI4KIIIα, as mutations in *fwd* and *PI4KII* affect Golgi but not PM morphology. Moreover, *PI4KIIIα* is required for normal levels of PM PtdIns4*P* and PtdIns(4,5)P_2. Because loss of *PI4KIIIα* phenocopies mutations in the PtdIns(4,5)P_2 regulators *sktl* and *Pten*, and titration of PtdIns(4,5)P_2 recapitulates *PI4KIIIα* mutant phenotypes, this suggests a crucial role for PI4KIIIα in synthesizing PtdIns4*P* that acts as a precursor to PtdIns(4,5)P_2. Our results highlight PI4KIIIα as a key regulator of cortical integrity and trafficking events at the PM, and emphasize that different pools of the same phosphoinositide can serve drastically different physiological and cellular functions.

RESULTS

PI4KIIIα is essential and allelic to *zeste-white 2*

To investigate the role of PI4KIIIα during *Drosophila* development, we generated a deletion in the corresponding gene. The deletion, henceforth referred to as *PI4KIIIα*$^{\Delta 123}$, removes the entire predicted kinase domain, the majority of the upstream phosphatidylinositol 3-kinase (PIK) accessory domain and part of the first exon of *shaggy* [*sgg*; also known as *zeste-white 3* (*zw3*); Fig. 1A; see Materials and Methods]. *PI4KIIIα*$^{\Delta 123}$ was recessive lethal, and hemizygous males died shortly after embryogenesis as first instar larvae. Lethality was due to disruption of *PI4KIIIα* because viability was fully rescued with a *PI4KIIIα* transgene (Fig. 1A).

PI4KIIIα is located at polytene interval 3A8 (Marygold et al., 2013). Because saturation mutagenesis had previously been performed in this region of the X chromosome, which lies between *zeste* and *white* (Judd et al., 1972), we tested *PI4KIIIα*$^{\Delta 123}$ for allelism to any of the previously identified lethal complementation groups. *PI4KIIIα*$^{\Delta 123}$ failed to complement *zeste-white 2*^{c21} [*zw2*^{c21}; also known as *lethal (1) 3Ah*^{21}, *l(1)3Ah*^{21}], but complemented *sgg* and *zw6*, two neighboring complementation groups (Fig. 1B). Like *PI4KIIIα*$^{\Delta 123}$, males hemizygous for *zw2*^{c21} or other *zw2* alleles die as first instar larvae (Shannon et al., 1972). These data indicate that *PI4KIIIα* is allelic to *zw2*. In addition, because *PI4KIIIα*$^{\Delta 123}$ complemented *sgg*, the small region of *sgg* removed in *PI4KIIIα*$^{\Delta 123}$ has no obvious effect on *sgg* function.

PI4KIIIα is required for normal egg chamber morphology

To determine whether a role for *PI4KIIIα* in embryogenesis was masked by a maternal contribution, female germline clones (GLCs) homozygous for *PI4KIIIα*$^{\Delta 123}$ were generated using the FLP-FRT system and the dominant female-sterile mutation *ovo*^{D} (Chou and Perrimon, 1992). No eggs were recovered upon induction of *PI4KIIIα*$^{\Delta 123}$ GLCs, consistent with a report that no embryos were produced when maternal *zw2* was eliminated (Perrimon et al., 1989). Hence, *PI4KIIIα* is required during oogenesis.

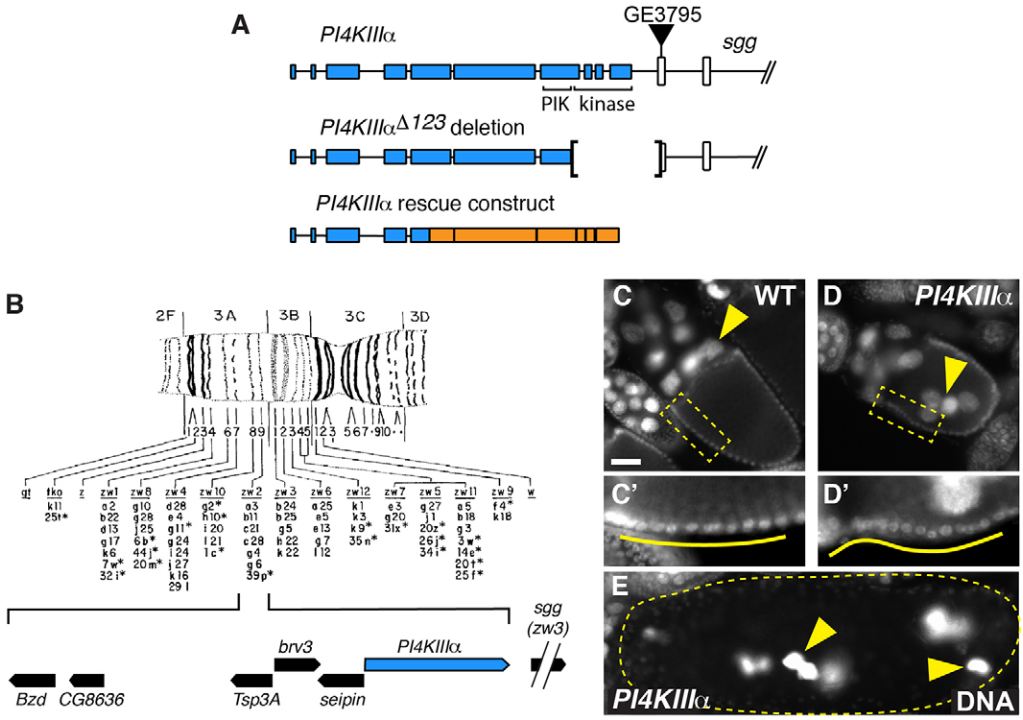

Fig. 1. *PI4KIIIα* is essential and required for oogenesis. (A) Schematic of *PI4KIIIα* (*CG10260*) locus (top), *PI4KIIIα*$^{\Delta 123}$ deletion (middle) and *PI4KIIIα* rescue construct (bottom). Blue bars, *PI4KIIIα* exons; white bars, *sgg* exons; orange bars, cDNA. *PI4KIIIα*$^{\Delta 123}$ was generated by imprecise excision of the P-element GE3785. (B) Physical location of *PI4KIIIα* within the region defined by the *zw2* complementation group [modified with permission, from Shannon et al. (Shannon et al., 1972)]. (C–E) Epifluorescence micrographs of egg chambers stained with DAPI to mark nuclei. Compared with WT (C), the oocyte cortex of *PI4KIIIα* GLCs (D) is buckled, as revealed by the position of follicle cell nuclei (boxed areas are enlarged 2.5× in C′,D′), and nurse cell nuclei are found in the ooplasm (D, arrowhead). (E) Late-stage GLCs exhibit pycnotic nuclei. Scale bar: 20 µm. Panels C′,D′ were adjusted similarly for brightness and contrast.

Journal of Cell Science (2014) 127, 954–966 doi:10.1242/jcs.129031

Examination of *PI4KIIIα*$^{\Delta 123}$ GLCs by DAPI staining revealed that in 50% of stage 9 or later egg chambers (n=36), nurse cell nuclei were found in the ooplasm, rather than being restricted to the anterior of the egg chamber (Fig. 1C,D). In addition, organization of the overlying layer of follicle cells appeared irregular, unlike the regular spacing observed in wild type (WT; Fig. 1C-D′). Mutant egg chambers at later stages showed evidence of border cell migration (see below) and nurse cell dumping (Fig. 1E), but lacked dorsal appendages (not shown). In addition, late-stage GLCs exhibited pycnotic nuclei (Fig. 1E) and appeared to degenerate.

PI4KIIIα is required for actin organization and Moesin activation

To understand the cellular basis for morphological defects in *PI4KIIIα*$^{\Delta 123}$ GLCs, egg chambers were stained with Rhodamine–phalloidin to visualize F-actin. In WT egg chambers, F-actin was found along the cortex of the germ cells and in ring canals (Fig. 2A,D). In early *PI4KIIIα*$^{\Delta 123}$ GLCs, cortical F-actin was greatly reduced and ring canals clustered towards the center of the cyst (Fig. 2C; Fig. 3D,F). These defects appeared to correlate, as cortical F-actin was observed in cysts where ring canals were not tightly coalesced into a single cluster (Fig. 2C) or were found in more than one cluster (Fig. 2B). Of GLCs with more than one cluster of ring canals, 92% (n=13) showed cortical F-actin, compared with 45% (n=33) in GLCs with one cluster. In late-stage *PI4KIIIα*$^{\Delta 123}$ GLCs, F-actin was present between some nurse cell nuclei but not others, and aggregations of F-actin often protruded into or across the oocyte (Fig. 2E). F-actin along the oocyte cortex was buckled and disorganized, in contrast to the smooth and rigid appearance of the WT cortex (Fig. 2D). These F-actin phenotypes were never observed in control GLCs from *ovo*^{D}/+ females and were rescued by the *PI4KIIIα* transgene, indicating that they are due to loss of *PI4KIIIα*

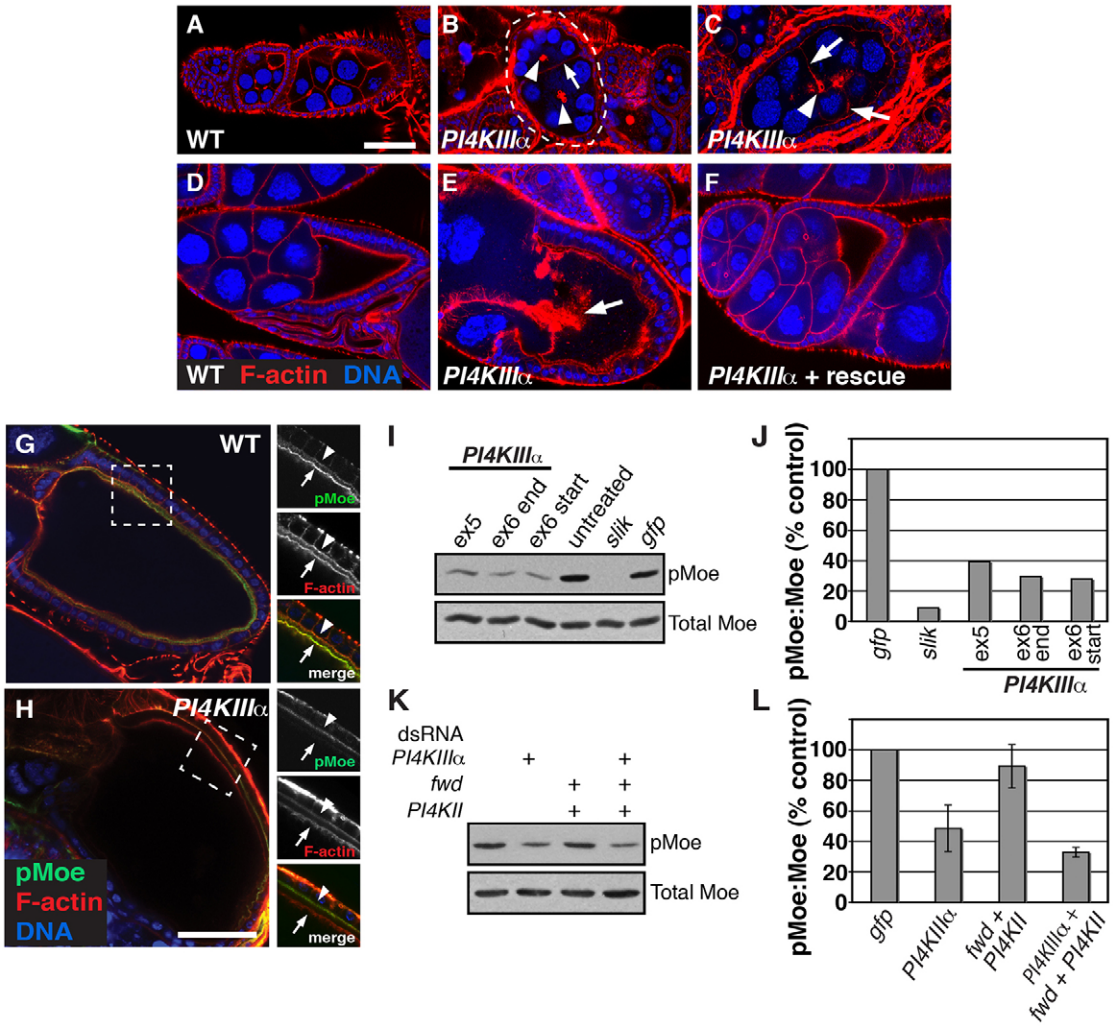

Fig. 2. *PI4KIIIα* mutant germlines display defects in F-actin organization and Moesin activation. (A–F) Confocal sections of early- (A–C) and late-stage (D–F) egg chambers stained for F-actin (Rhodamine–phalloidin; red) and DNA (ToPro; blue). Early *PI4KIIIα* GLCs have reduced cortical F-actin (B,C, arrows) and clustered ring canals (arrowheads), whereas late-stage GLCs have F-actin protrusions (E, arrow). Dashed line (B) indicates a single egg chamber. (F) Actin defects are rescued by a *PI4KIIIα* rescue construct. (G,H) Confocal micrographs of egg chambers stained with anti-pMoe (green), Rhodamine–phalloidin (red) and ToPro (blue). Right panels are 2×-magnified views of the boxed areas, showing the oocyte cortex (arrows) and the apical side of the follicular epithelium (arrowheads). Compared with WT (G), pMoe is severely reduced in *PI4KIIIα* GLCs (H, arrows), but not in the apical regions of follicle cells (H, arrowheads). (I–L) Immunoblotting of lysates from dsRNA-treated S2 cells (I,K) and quantification of immunoblots (J,L). Depletion of *PI4KIIIα* with any of three dsRNAs reduces pMoe levels without affecting total Moe protein levels (I,J). Co-depletion of *fwd* and *PI4KII* has little effect on pMoe levels (K,L). *slik* and *gfp* dsRNAs serve as positive and negative controls, respectively. Scale bars: 50 μm.

Journal of Cell Science (2014) 127, 954–966 doi:10.1242/jcs.129031

(Fig. 2F; 100% penetrance in rescuing viability, fertility and F-actin phenotypes).

Delamination of F-actin from the PM suggested a possible defect in crosslinking the cortical cytoskeleton to the overlying membrane (Jankovics et al., 2002; Polesello et al., 2002; Verdier et al., 2006). Because phosphorylation of the cytoskeletal–membrane crosslinker Moesin (Moe) is required to maintain cortical actin in the oocyte, and PtdIns(4,5)P_2 binding is required for Moe phosphorylation (Fievet et al., 2004; Roch et al., 2010), we examined localization of activated, phosphorylated Moe (pMoe) in *PI4KIIIα*$^{\Delta 123}$ GLCs. In WT stage 10B egg chambers, pMoe colocalized with F-actin along both the oocyte PM and the juxtaposed apical membranes of follicle cells (Fig. 2G). In similarly staged *PI4KIIIα*$^{\Delta 123}$ GLCs, pMoe was greatly reduced at the oocyte cortex and F-actin was more diffuse (Fig. 2G,H), whereas apical localization of pMoe and F-actin appeared normal in adjacent follicle cells (Fig. 2G,H).

To examine whether loss of *PI4KIIIα* affected overall levels of pMoe in addition to pMoe localization, *Drosophila* S2 cells were treated with double-stranded RNAs (dsRNAs) to knock down *PI4KIIIα* expression by RNA interference (RNAi) and levels of pMoe were assessed by immunoblotting. Treatment with any of three non-overlapping *PI4KIIIα* dsRNAs reduced the amount of pMoe to ~25–40% compared to mock treatment or RNAi directed against green fluorescent protein (GFP), but was not as dramatic as RNAi directed against the Moe kinase Slik (Hipfner et al., 2004) (Fig. 2I,J). Total levels of Moe remained unchanged, demonstrating that PI4KIIIα does not affect Moe production or stability. The effect on pMoe levels was specific to *PI4KIIIα*, as RNAi directed against the other *Drosophila* PI4Ks, *fwd* and *PI4KII*, had no effect (Fig. 2K,L; supplementary material Fig. S1). In immunofluorescence experiments, pMoe levels were slightly reduced at the cortex of stage 10B *fwd* mutant oocytes (supplementary material Fig. S2B). However, no actin defects were observed in *fwd* egg chambers (see below). pMoe localization in *PI4KII* mutant oocytes resembled WT (supplementary material Fig. S2C). Depletion of the phosphatidylinositol 4-phosphate 5-kinase (PIP5K) Skittles (Sktl), which converts PtdIns4*P* to PtdIns(4,5)P_2, also blocked pMoe accumulation in S2 cells (Roubinet et al., 2011) (supplementary material Fig. S2D,E).

PI4KIIIα is required for plasma membrane integrity and exocyst localization

The presence of nurse cell nuclei in the ooplasm suggested that membrane barriers might be compromised in *PI4KIIIα*$^{\Delta 123}$ GLCs. To examine PM integrity in early- and late-stage egg chambers, membranes were visualized using fluorophore-conjugated tomato lectin, which binds glycoproteins on intracellular and cell surface membranes (Dollar et al., 2002; Murthy and Schwarz, 2004; Verdier et al., 2006). In early WT egg chambers, lectin-positive membranes largely colocalized with cortical F-actin (Fig. 3A,B). In contrast, early-stage *PI4KIIIα*$^{\Delta 123}$ GLCs displayed thinner, discontinuous lectin staining along membranes (Fig. 3C,D), as well as lectin-positive aggregates within the cytoplasm, often concentrated near clustered ring canals (Fig. 3C,D). Thinner lectin staining reflected loss of PM, which was evident in transmission electron micrographs. In contrast to prominent membranes separating WT nurse cell nuclei (Fig. 3G–I), *PI4KIIIα*$^{\Delta 123}$ GLCs had vesiculated membranes around clustered ring canals (Fig. 3J), thin membranes between some nurse cell nuclei (Fig. 3K,L), and none between others (Fig. 3K). In addition, membranes terminated within the cytoplasm in *PI4KIIIα*$^{\Delta 123}$ GLCs (Fig. 3K,L). Loss of cortical F-actin paralleled loss of membranes; seven out of eight GLCs with cortical F-actin between germ cell nuclei also had overlying membrane (Fig. 3D). In early egg chambers with more severe phenotypes, the somatic follicular epithelium that normally encapsulates the cyst also degenerated or was missing (Fig. 3E,F). This somatic phenotype could be an indirect effect of the germline on the follicle cells, or could result from defects due to the presence of unmarked mutant follicle cell clones. Thus, only GLCs with an intact follicular epithelium and the presence of cortical F-actin were scored as mildly affected (52%, $n=58$). In late-stage GLCs, membranes were seen between some nuclei but not others (Fig. 4A,B), and at times formed a large whorl that colocalized with F-actin in the oocyte (Fig. 4B). These effects were specific to *PI4KIIIα* GLCs, as *fwd* and *PI4KII* mutant egg chambers showed distinct phenotypes (Fig. 4C,D; see below). Given the presence of membranes and evidence of border cell migration in some late-stage GLCs (Fig. 4B), we hypothesize that mildly affected early mutant GLCs are able to mature to late stages, whereas severely affected early GLCs (e.g. Fig. 3F) fail to survive.

Because lack of cortical F-actin, clustering of ring canals and disintegration of PM are also seen in GLCs homozygous for mutations that affect membrane addition, including the exocyst subunits Sec5 and Sec6 (Beronja et al., 2005; Murthy et al., 2005; Murthy and Schwarz, 2004), we examined Sec5 distribution. In WT stage 6–8 egg chambers, Sec5 was found at the PM and was enriched on oocyte membranes (Murthy and Schwarz, 2004) (Fig. 5A,B). In *PI4KIIIα*$^{\Delta 123}$ GLCs, this localization was lost, even in mildly affected egg chambers that retained cortical F-actin (Fig. 5D,E). Sec5 was reduced on both the oocyte and nurse cell membranes (Fig. 5B,E). In contrast to WT (Fig. 5C), the level of Sec5 at the oocyte–follicle cell interface in *PI4KIIIα* GLCs (Fig. 5F) was no stronger than on lateral follicle cell membranes, indicating that *PI4KIIIα* GLCs fail to recruit or retain the exocyst.

PI4KIIIα, *fwd* and *PI4KII* have differential effects on cellular membranes

To test whether the observed PM defects result from a specific requirement for PI4KIIIα or a general requirement for PtdIns4*P*, we examined egg chambers in *fwd* and *PI4KII* null mutants. Overall, the PM was intact and F-actin appeared normal (Fig. 4C,D), indicating that actin organization and PM integrity during oogenesis do not require Fwd or PI4KII. Additionally, Sec5 localization was not affected in *fwd* or *PI4KII* mutants (supplementary material Fig. S3). However, in late-stage *fwd* and *PI4KII* egg chambers, nurse cells showed large lectin-positive structures in the cytoplasm (Fig. 4C,D) that were not visible in late-stage WT egg chambers or *PI4KIIIα*$^{\Delta 123}$ GLCs (Fig. 4A,B). These structures were more prominent in *PI4KII* than *fwd* mutants, with large puncta visible in early *PI4KII* egg chambers that had otherwise normal lectin staining (Fig. 6D).

To further define these intracellular membrane defects, *PI4KIIIα*$^{\Delta 123}$ GLCs and *fwd* and *PI4KII* mutant egg chambers were immunostained for the cis-Golgi marker Lava lamp (Lva). In stage 7 or earlier WT egg chambers, Lva decorated discrete puncta in the cytoplasm of germ cells, with ~40% of Lva structures partially overlapping with lectin puncta and vice versa (Fig. 6A,F). Lva puncta varied in size, with larger Lva structures

Journal of Cell Science (2014) 127, 954–966 doi:10.1242/jcs.129031

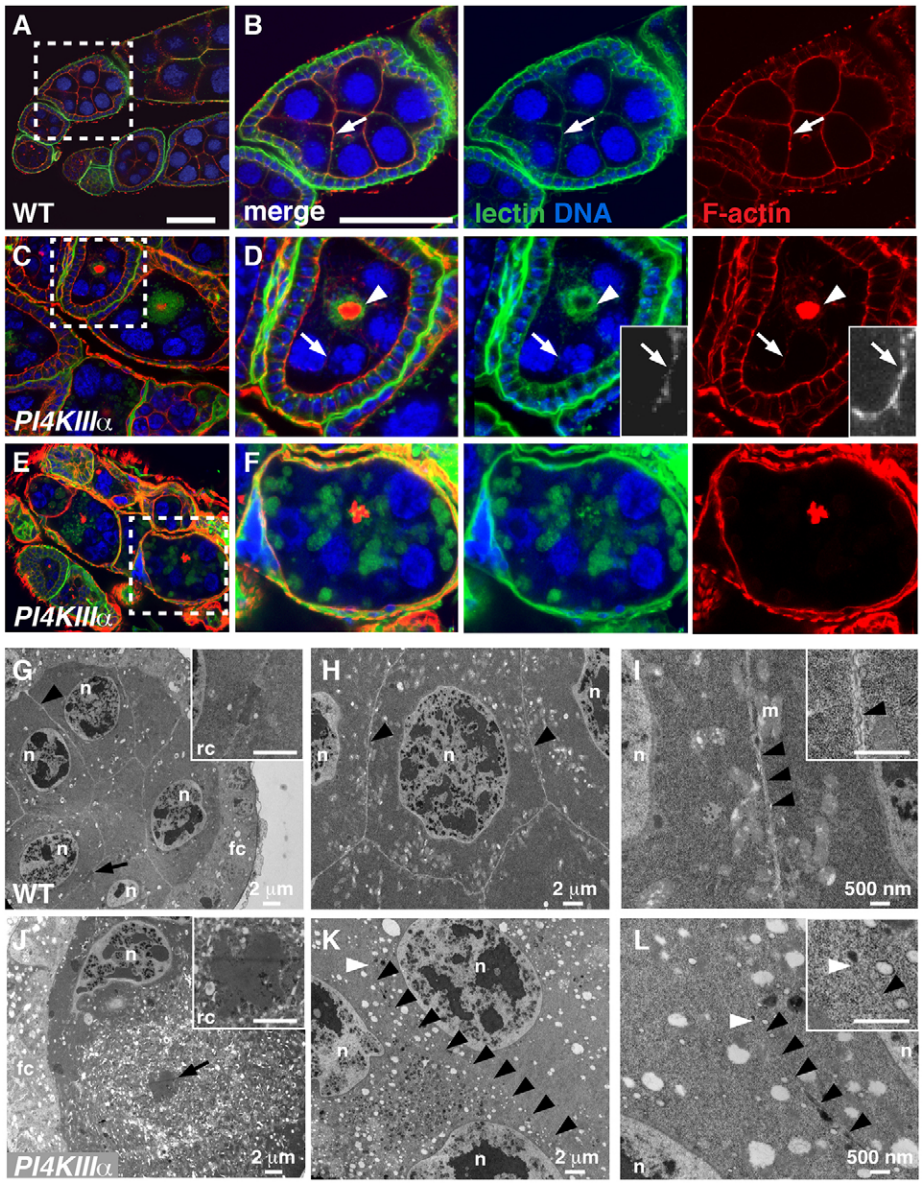

Fig. 3. Membrane integrity is defective in *PI4KIIIα* germline clones. (A–F) Confocal sections of early-stage egg chambers stained with fluorescein–tomato lectin (green), Rhodamine–phalloidin (red) and ToPro (blue). Boxed areas in A,C,E are enlarged in B,D,F. Insets in D are magnified 3× and adjusted for brightness and contrast. In WT (A,B), lectin staining marks the PM and colocalizes with cortical F-actin (B, arrows). In contrast, *PI4KIIIα* GLCs (C–F) show reduced lectin staining along the PM and decreased cortical F-actin (D, arrows, insets), whereas the remaining lectin-positive membrane localizes around the cluster of ring canals (D, arrowheads). In severely affected egg chambers (E,F), aggregates of membrane are found throughout the egg chamber and follicle cells appear to degenerate (F). Scale bars: 50 μm. (G–L) Transmission electron micrographs of WT (G–I) and *PI4KIIIα* GLCs (J–L). Stage 5 egg chambers showing a single ring canal in WT (G) and a cluster of ring canals in a *PI4KIIIα* GLC (J, arrows; compare insets). Stage 7 egg chambers show a robust PM separating each nurse cell nucleus in WT (H,I, arrowheads), but thin (K,L, black arrowheads) or no (K, bottom two nuclei) PM between nuclei of *PI4KIIIα* GLCs. Thin membranes in *PI4KIIIα* terminate within the cytoplasm (K,L, white arrowheads). Inset in I is from a different region of the same egg chamber. fc, follicle cell; m, mitochondria; n, nurse cell nucleus; rc, ring canal(s).

being associated with larger lectin-positive structures (Fig. 6A, compare boxes 1–3). In contrast, *fwd* and *PI4KII* mutant egg chambers showed obvious, yet distinct, defects in Golgi morphology. In *fwd* mutants, Lva puncta were significantly smaller than WT (Fig. 6C,E). Lectin puncta that partially overlapped with larger Lva puncta were either irregularly shaped (Fig. 6C, box 1) or elongated (Fig. 6C, box 2); 22.4% (n=241) of *fwd* puncta were abnormally shaped compared with 8.5% in WT (n=188) and 7.8% in *PI4KII* (n=90). Many of the small Lva puncta appeared to be in close proximity to, but did not overlap with, small lectin puncta (Fig. 6C, box 3). As tomato lectin is predicted to bind glycosylated proteins at the trans-Golgi network (TGN), this may indicate fragmentation of the TGN. Lva puncta in *PI4KII* were slightly larger and more varied in size (Fig. 6D,E). The largest structures were often still associated with lectin, but many appeared to be clusters of several Lva puncta that could not be resolved at the level of confocal microscopy (Fig. 6D, inset 1). Within some clusters, discrete Lva puncta were distinguishable and scored as separate units (Fig. 6D, box 3; scored as three Lva bodies). Overall, the average numbers of Lva puncta in *fwd* (112.3±17.5; mean ± s.e.m.) and *PI4KII* (114.0±1.4) egg chambers were similar to WT (124.7±58.8; n=2–3 egg chambers each). These results suggest *fwd* and *PI4KII* affect Golgi morphology and the manner in which cis-Golgi associate with the TGN.

In contrast, in *PI4KIIIα*$^{\Delta 123}$ GLCs, Lva puncta were of similar size, shape and number (118.7±28.7 per GLC, n=3) to those in WT (Fig. 6E), and appeared as individual units rather than clusters. Lva puncta located away from the center cluster partially overlapped with adjacent lectin puncta, as in WT (Fig. 6B, boxes 1–3). However, in contrast to the perinuclear localization of Golgi in WT, most Lva puncta were localized to the center of the cyst near the clustered lectin-positive membranes (Fig. 6B). This may be a secondary consequence of PM breakdown, as other organelles were concentrated in this region as well (Fig. 3J and not shown). Membrane clustering made it difficult to assess specific association between lectin and Lva puncta. Although the normal size, shape and number of Lva puncta suggest that cis-Golgi morphology is not grossly affected in the absence of PI4KIIIα, inability to assess most of the lectin puncta precludes a

Journal of Cell Science (2014) 127, 954–966 doi:10.1242/jcs.129031

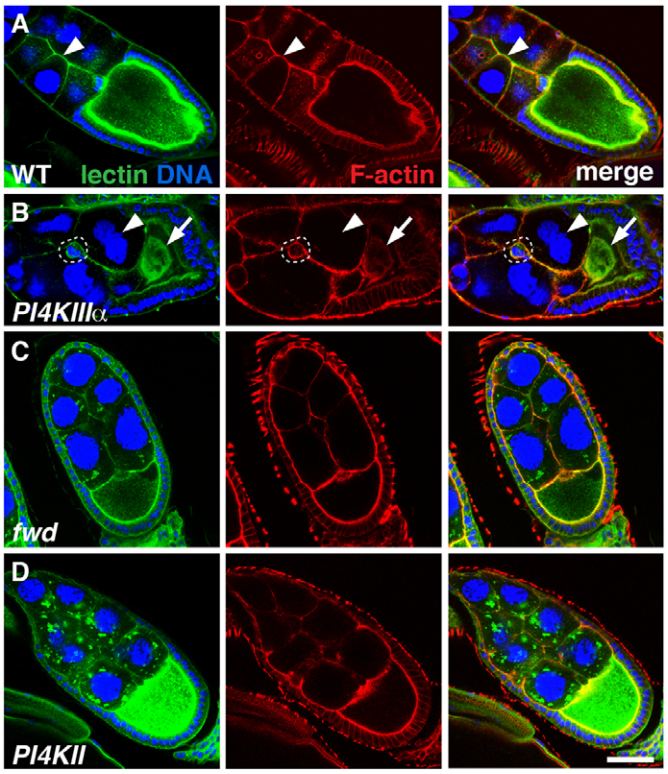

Fig. 4. *PI4KIIIα* germline clones exhibit membrane defects not seen in other PI4K mutants. (A,B) Confocal micrographs of a late-stage WT egg chamber (A) and a *PI4KIIIα* GLC (B) stained with fluorescein–lectin (green), Rhodamine–phalloidin (red) and ToPro (blue). Compared with WT (A, arrowheads), nurse cell membranes are disrupted or missing in *PI4KIIIα* GLCs (B, arrowheads) and a whorl of membrane colocalizes with F-actin in the oocyte (arrows). Border cells, dashed circles. (C,D) Confocal sections of *fwd* (C) and *PI4KII* (D) mutant egg chambers stained with Texas-Red–lectin (green), Alexa-Fluor-488–phalloidin (red) and ToPro (blue). In contrast to *PI4KIIIα* GLCs (B), *fwd* and *PI4KII* nurse cell membranes are intact. However, prominent membrane aggregates are found in the nurse cell cytoplasm. Scale bar: 50 μm.

conclusion about the effect of $PI4KIII\alpha^{\Delta 123}$ on overall Golgi organization.

PI4KIIIα is required for PM PtdIns4*P* and PtdIns(4,5)P_2

Because $PI4KIII\alpha^{\Delta 123}$ had drastic effects on the PM and actin cytoskeleton, we reasoned that *PI4KIIIα* might affect PM levels of PtdIns4*P* or PtdIns(4,5)P_2. To detect PtdIns(4,5)P_2, we examined PLCδPH–GFP, a fluorescent reporter that has also been used to titrate PtdIns(4,5)P_2 (Raucher et al., 2000). Low-level ubiquitous expression of PLCδPH–GFP marked the PM and colocalized with cortical F-actin in WT developing egg chambers (Fig. 7A,B). However, 50% of the egg chambers exhibited nurse cell nuclei in the ooplasm, indicating that titration of PtdIns(4,5)P_2 can recapitulate a $PI4KIII\alpha^{\Delta 123}$ phenotype (Fig. 7B).

To assess PM phosphoinositide levels without eliciting phenotypes by titration, we used anti-PtdIns4*P* or anti-PtdIns(4,5)P_2 antibodies to immunostain WT egg chambers and $PI4KIII\alpha^{\Delta 123}$ GLCs. In WT, PtdIns4*P* was detected along the PM and in ring canals (Fig. 7C). In contrast, $PI4KIII\alpha^{\Delta 123}$ GLCs showed reduced PtdIns4*P* staining at the PM (Fig. 7D; 76.7% of egg chambers, $n=30$). Because PM integrity is compromised in $PI4KIII\alpha^{\Delta 123}$ GLCs, reduced PtdIns4*P* staining might be due to loss of membranes. To account for this, we examined the PtdIns4*P* signal in relation to cortical F-actin. If the decrease in PtdIns4*P* staining intensity was due to loss of membrane, and not a decrease in the level of PtdIns4*P*, we would expect GLCs to exhibit a PtdIns4*P*:F-actin ratio similar to that in WT. However, of the GLCs that showed reduced PtdIns4*P*, the average PtdIns4*P*:F-actin ratio was 55.5% of WT (Fig. 7E; $n=23$, $P<0.01$), indicating that *PI4KIIIα* controls PtdIns4*P* levels at the PM. Similar to PtdIns4*P*, PtdIns(4,5)P_2 was detected along the PM and in ring canals in WT (Fig. 7F). PtdIns(4,5)P_2 was also reduced in *PI4KIIIα* GLCs, although to a lesser extent (Fig. 7G; 46.9% of egg chambers, $n=49$); the PtdIns(4,5)P_2:F-actin ratio was 70.5% of WT (Fig. 7H; $n=23$, $P<0.05$). Thus, PI4KIIIα is needed for normal PtdIns4*P* and PtdIns(4,5)P_2 levels at the PM.

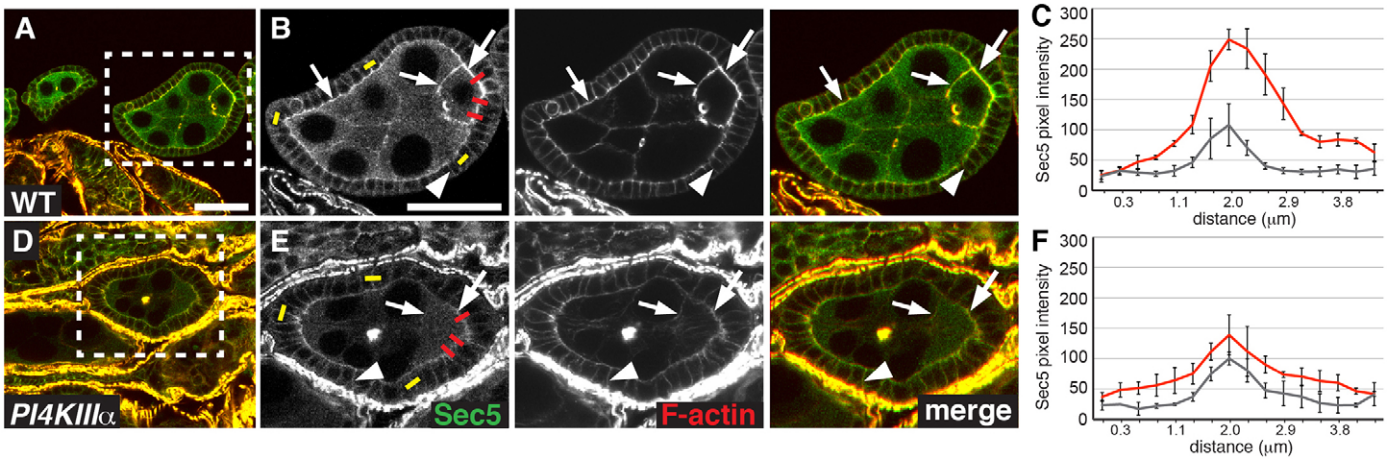

Fig. 5. Loss of *PI4KIIIα* disrupts Sec5 localization. (A,B,D,E) Confocal micrographs of egg chambers stained with anti-Sec5 (green) and Rhodamine–phalloidin (red). Boxed areas in A,D are enlarged in B,E. In WT, Sec5 is enriched at the oocyte PM and along nurse cell membranes adjacent to follicle cells (B, arrows). In *PI4KIIIα* GLCs, Sec5 at these membranes is lost, i.e. the Sec5 signal at the nurse-cell–follicle-cell interface is similar to that in lateral follicle cell membranes (E, compare arrows, arrowheads). Scale bars: 50 μm. (C,F) Quantification of Sec5 intensity across the lateral follicle cell membranes (gray; average intensity taken from positions indicated by yellow bars in B and E) and across the oocyte-posterior follicle cell membranes (red; average intensity taken from positions indicated by red bars in B and E) for WT (C) and *PI4KIIIα* (F). Bars indicate standard deviations.

Journal of Cell Science (2014) 127, 954–966 doi:10.1242/jcs.129031

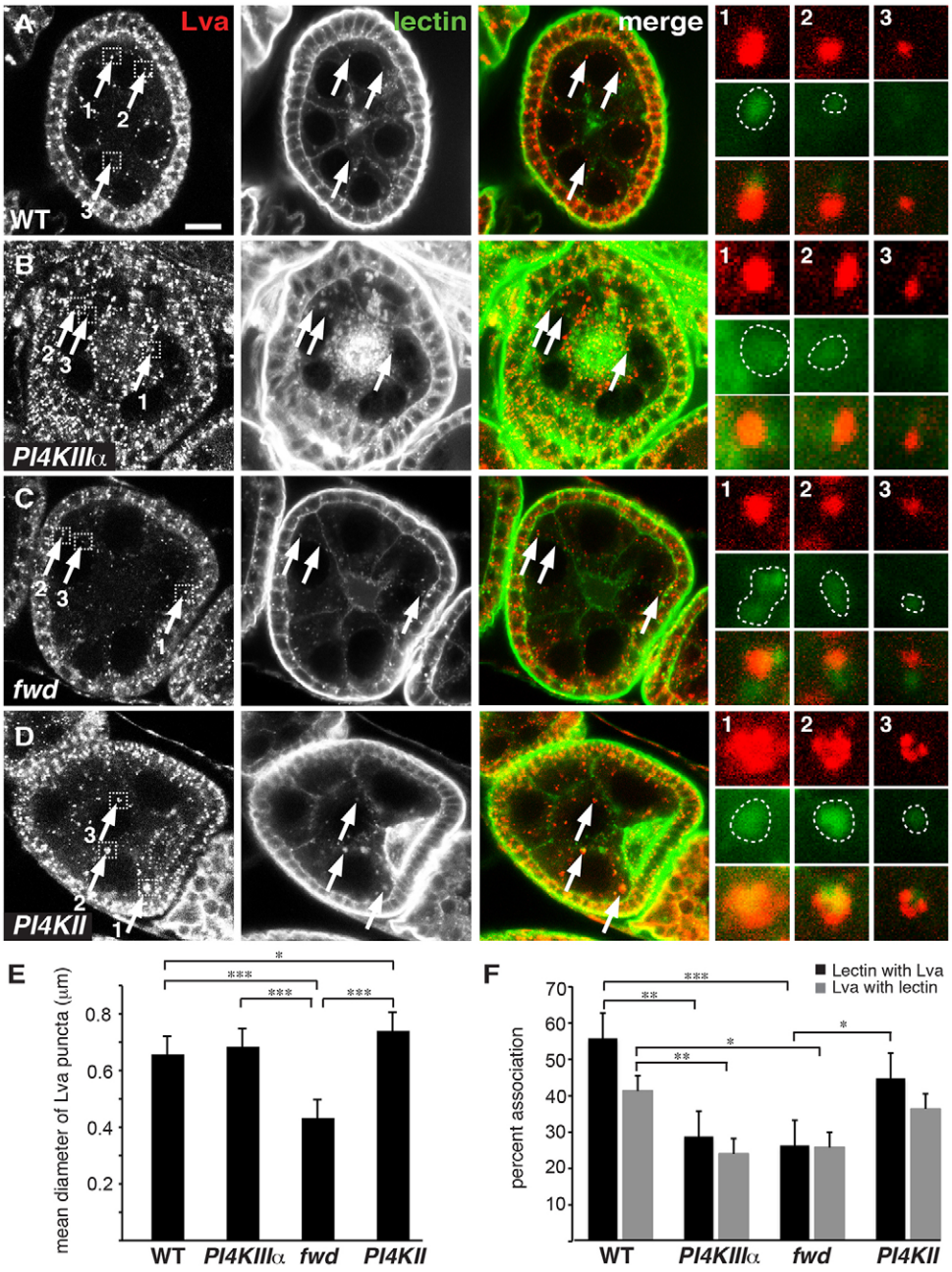

Fig. 6. Fwd and PI4KII regulate Golgi morphology and organization. (A–D) Confocal images of egg chambers stained with anti-Lva (red) and fluorescein–tomato lectin (green). Images at far right are 8× enlargements of boxed areas 1, 2 and 3. Dotted lines trace the shape of lectin puncta, where discernible. (A) Discrete Lva puncta are visible in WT egg chambers and partially colocalize to lectin-positive puncta. The sizes of Lva puncta were proportional to the sizes of lectin puncta (boxes 1–3); small Lva puncta had either barely discernible or no adjacent lectin puncta (box 3). (B) Lectin-positive membranes in *PI4KIIIα* GLCs accumulate towards the center of the egg chamber. Elsewhere, the sizes of Lva and associated lectin puncta resemble those in WT, although the lectin puncta appear more diffuse (boxes 1–3). (C) *fwd* egg chambers have smaller Lva puncta that overlap more with either irregularly shaped (box 1) or elongated (box 2) lectin puncta. The smallest Lva puncta were either not associated with lectin or were in close proximity to, but not overlapping with, small lectin puncta (box 3). (D) Lva puncta in *PI4KII* mutants overlap with engorged lectin puncta (boxes 1, 2). Often, several Lva puncta associate with a single lectin spot (boxes 1–3). (E) Mean diameter of individual Lva puncta found in egg chambers of the genotypes listed. WT, $n=251$ puncta (3 egg chambers); *PI4KIIIα*, $n=554$ (6 egg chambers); *fwd*, $n=399$ (4 egg chambers); *PI4KII*, $n=132$ (2 egg chambers). (F) Percentage colocalization of lectin puncta with Lva (black bars) and Lva puncta with lectin (gray bars). WT, $n=388$ lectin and 374 Lva puncta (3 egg chambers); *PI4KIIIα*, $n=291$ lectin and 356 Lva puncta (3 egg chambers); *fwd*, $n=436$ lectin and 337 Lva puncta (3 egg chambers); *PI4KII*, $n=139$ lectin and 228 Lva puncta (2 egg chambers). Bars indicate standard error. $^{*}P<0.05$, $^{**}P<0.01$, $^{***}P<0.001$. Scale bar: 10 μm.

PI4KIIIα is required for egg chamber polarity

Egg chambers with reduced levels of PtdIns(4,5)P_2, as a result of mutation of the PIP5K Sktl, have oocyte polarity defects (Gervais et al., 2008). Thus, we examined whether *PI4KIIIα*$^{\Delta 123}$ GLCs also exhibit polarity defects. Oskar is localized to the posterior pole in stage 9 or later WT egg chambers (Fig. 8A,A′). In *PI4KIIIα*$^{\Delta 123}$ GLCs, Oskar was either reduced (Fig. 8B,B′) or missing (Fig. 8C,C′) at the posterior pole, correlating with the degree of F-actin disruption. Two other polarity indicators are successful migration of the oocyte nucleus and localization of Gurken to the dorsal–anterior of the oocyte at stage 8 (Roth, et al., 1995) (Fig. 8D). In *PI4KIIIα*$^{\Delta 123}$ GLCs, Gurken was either not visibly concentrated within the egg chamber (Fig. 8E) or not associated with the oocyte nucleus (Fig. 8F). In addition, the oocyte nucleus failed to localize at the dorsal–anterior position (3/8 were properly localized, compared with 10/10 in WT) (Fig. 8D,F,G, asterisks; quantified in Fig. 8H). Hence, *PI4KIIIα*$^{\Delta 123}$ phenocopies *sktl* polarity defects.

DISCUSSION

Many cellular processes at the PM depend on phosphoinositides, although it has remained unclear whether these processes are coordinately regulated. Here, we show that during oogenesis, PI4KIIIα is essential for coordinating membrane trafficking and actin organization at the cortex, as well as for integrity of the PM itself. Furthermore, our data suggest that PI4KIIIα is the PI4K that affects PM phosphoinositides. We provide several lines of evidence indicating that a major role for this enzyme is production of PtdIns4*P* for conversion into PtdIns(4,5)P_2 at the PM.

First, *PI4KIIIα*$^{\Delta 123}$ GLCs exhibit nurse cell nuclei in the ooplasm and accumulation of intracellular F-actin, distinctive

Journal of Cell Science (2014) 127, 954–966 doi:10.1242/jcs.129031

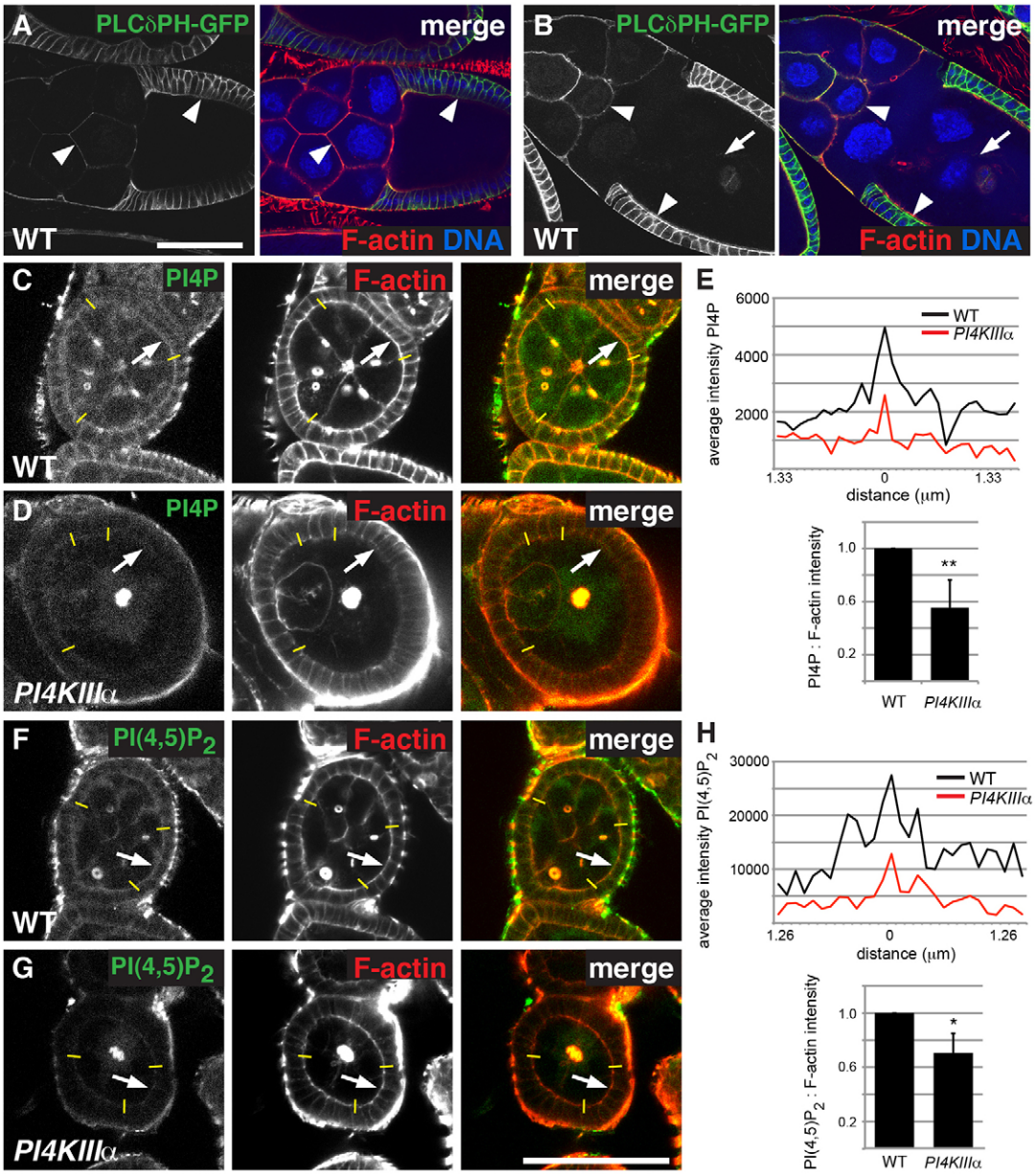

Fig. 7. *PI4KIIIα* is required for plasma membrane PtdIns4*P* and PtdIns(4,5)P_2. (A,B) Confocal sections of WT egg chambers expressing the PtdIns(4,5)P_2 marker PLCδPH–GFP under control of α_1-tubulin-GAL4 (green) and stained with Rhodamine–phalloidin (red) and ToPro (blue). PLCδPH–GFP labels the PM and colocalizes with F-actin (A,B, arrowheads). Approximately 50% of these egg chambers have nurse cell nuclei within the ooplasm, similar to *PI4KIIIα* GLCs (B, arrow). (C,D,F,G) WT egg chambers (C,F) or *PI4KIIIα* GLCs (D,G) stained with anti-PtdIns4*P* (PI4P; C,D) or anti-PtdIns(4,5)P_2 [PI(4,5)P_2; F,G] antibodies (green) and Rhodamine–phalloidin (red). PtdIns4*P* and PtdIns(4,5)P_2 are detected on the PM (arrows) and in ring canals. Overall intensities of PtdIns4*P* and PtdIns(4,5)P_2 were reduced along the PM in *PI4KIIIα* GLCs compared with WT (compare arrows in C with D, F with G). (E,H) Top: representative plot of average intensity of PtdIns4*P* (E) or PtdIns(4,5)P_2 (H) staining in WT egg chamber (black line) compared with *PI4KIIIα* GLC (red line). Average intensity was plotted using values taken from positions indicated by yellow bars in C,D (for E) and in F,G (for H). Bottom: average PtdIns4*P*:F-actin (E, n=23; 76.7% of egg chambers examined) and PtdIns(4,5)P_2:F-actin (H, n=23; 46.9% of egg chambers examined) intensity ratios normalized to WT. *P<0.05, **P<0.001. Scale bars: 50 μm.

phenotypes also observed in GLCs mutant for the PtdIns(3,4,5)P_3 phosphatase Pten (von Stein et al., 2005), loss of which would also result in decreased levels of PtdIns(4,5)P_2. The similar phenotypes of *PI4KIIIα* and *Drosophila Pten* mutants strongly suggest they impinge upon a common pool of PtdIns(4,5)P_2. Second, ubiquitous expression of PLCδPH–GFP, which titrates PtdIns(4,5)P_2, recapitulated this phenotype in 50% of otherwise WT egg chambers. Third, immunostaining revealed reduced levels of PtdIns4*P* and PtdIns(4,5)P_2 in the PM of *PI4KIIIα* GLCs. Fourth, *PI4KIIIα* GLCs fail to activate and recruit proteins known to require PtdIns(4,5)P_2. pMoe was dramatically reduced at the oocyte cortex in GLCs, and Moe phosphorylation was attenuated in *PI4KIIIα* knockdown cells. Additionally, *PI4KIIIα* GLCs failed to recruit or retain the exocyst subunit Sec5 at the PM. Indeed, *PI4KIIIα* GLCs phenocopy the disruption of cortical F-actin seen in mutants for Moe and the Moe activator dRok, and exhibit PM defects found in GLCs mutant for the exocyst subunits Sec5 and Sec6, as well as Rab6, a regulator of secretion, and Rab11, which binds the exocyst component Sec15 to promote vesicle recycling (Bogard et al., 2007; Coutelis and Ephrussi,

Journal of Cell Science (2014) 127, 954–966 doi:10.1242/jcs.129031

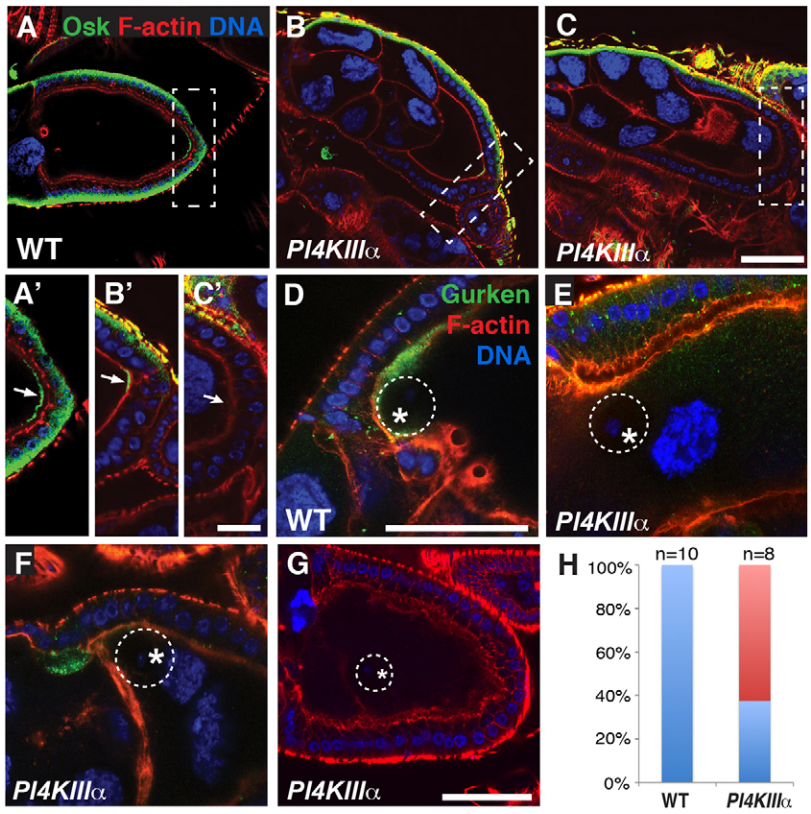

Fig. 8. Polarity defects in *PI4KIIIα* GLCs. (A–C) Egg chambers stained with anti-Oskar antibodies (green), Rhodamine–phalloidin (red) and ToPro (blue). (A′,B′,C′) 2×-magnified views of boxed areas. Oskar protein is concentrated at the posterior of the oocyte in stage 9 or later egg chambers in WT (A′, arrow), but is either reduced or absent in *PI4KIIIα* (B′,C′, arrows). Variability of Oskar localization in *PI4KIIIα* correlated with the degree of F-actin disruption throughout the rest of the egg chamber (compare Rhodamine–phalloidin in B,C). Oskar staining of the follicle cells is non-specific. (D–F) Egg chambers stained with anti-Gurken (green), Rhodamine–phalloidin (red) and ToPro (blue). (D) In WT, Gurken is found directly above the oocyte nucleus, which is anchored in the dorsal anterior corner of the oocyte in stage 10 egg chambers (outline, asterisk). In *PI4KIIIα* oocytes with an anchored nucleus, Gurken is either dispersed (E) or mislocalized (F) relative to the oocyte nucleus. (G) *PI4KIIIα* egg chamber with mislocalized oocyte nucleus. (H) Frequency of normal (blue bar) and abnormal (red bar) nuclear position in WT versus *PI4KIIIα* oocytes. Scale bars: 50 μm (A–G).

2007; Jankovics et al., 2002; Januschke et al., 2007; Langevin et al., 2005; Murthy et al., 2005; Polesello et al., 2002; Verdier et al., 2006; Wu et al., 2005). Thus, *PI4KIIIα*, by synthesizing the precursor to PtdIns(4,5)P_2, exerts profound effects on PM signaling and stability.

Consistent with this, *PI4KIIIα*$^{\Delta 123}$ GLCs resemble GLCs for the PIP5K Sktl. For example, pMoe localization is also defective in *sktl* hypomorphic GLCs (Gervais et al., 2008). However, *PI4KIIIα* oogenesis defects are not identical to those of *sktl*. Although marked GLCs of *sktl* null alleles have been reported (Gervais et al., 2008), *PI4KIIIα*$^{\Delta 123}$ GLCs made in this manner fail to thrive among WT follicles (our unpublished observations). This suggests that Sktl is at least partially redundant with another *Drosophila* PIP5K during oogenesis. Support for this idea stems from observations that PI4KIIIα and PI5K59B carry out similar functions in Rho activation during mesoderm migration (Murray et al., 2012), and that expression of dominant-negative versions of Rho GTPase family members during oogenesis causes aggregation of ring canals and loss of cortical F-actin, similar to *PI4KIIIα*$^{\Delta 123}$ GLCs (Murphy and Montell, 1996). Hence, we suggest that in *Drosophila* oogenesis PI4KIIIα acts upstream of Sktl, and perhaps also PIP5K59B, to produce a pool of PtdIns4*P* that feeds PM PtdIns(4,5)P_2.

Loss of *PI4KIIIα* has a greater effect on PtdIns4*P* than on PtdIns(4,5)P_2; a smaller percentage of GLCs showed reduced PtdIns(4,5)P_2, and those that did were less strongly affected. Interestingly, in *PI4KIIIα* knockout MEFs, PtdIns4*P* and PtdIns(4,5)P_2 reporters are dramatically reduced at the PM, whereas global levels of PtdIns(4,5)P_2 are only modestly affected when assessed by metabolic labeling (Nakatsu et al., 2012). This is probably due to the observed upregulation of two PIP5Ks, PIPKIβ and PIPK1γ. Hence, it is possible that compensatory upregulation of *Drosophila* PIP5Ks accounts for the weaker effect of *PI4KIIIα* on PtdIns(4,5)P_2. Alternatively, in the absence of PI4KIIIα, one of the other PI4Ks could supply a small amount of PtdIns4*P* that serves as a precursor to PtdIns(4,5)P_2.

Our results leave open the possibility of PtdIns(4,5)P_2-independent functions for PM PtdIns4*P*. It is noteworthy that some functions previously attributed to PM PtdIns(4,5)P_2 were found to be reliant on a negative charge that could be provided by either PtdIns4*P* or PtdIns(4,5)P_2 (Hammond et al., 2012). Thus, in *PI4KIIIα*$^{\Delta 123}$ GLCs, it is possible that lack of PtdIns4*P* is directly responsible for some of the observed phenotypes. However, the fact that *sktl* GLCs show similar phenotypes indicates that either PtdIns4*P* alone is not sufficient or that PtdIns(4,5)P_2 is specifically required. Because PI4KIIIα regulates both PtdIns4*P* and PtdIns(4,5)P_2, the mechanism by which PtdIns4*P* contributes to PM function in *Drosophila*, whether as a direct regulator, a precursor, or both, remains an open question.

Several aspects of cell polarity were disrupted in *PI4KIIIα*$^{\Delta 123}$ GLCs. Failure of the oocyte nucleus to migrate or anchor at the dorsal-anterior and mislocalization of Gurken are phenotypes shared with *sktl* mutants (Gervais et al., 2008). Oskar protein was either reduced or missing from the posterior pole, suggesting *PI4KIIIα*, like *sktl* and *Pten*, may also affect *oskar* mRNA localization (Gervais et al., 2008; von Stein et al., 2005). A similar effect on *oskar* mRNA and protein was frequently observed in *moesin* mutant egg chambers (Jankovics et al., 2002; Polesello et al., 2002). We noted that the extent of the Oskar defect correlated with the degree of F-actin disruption, suggesting that the effect of PI4KIIIα on Oskar is mediated in part through Moesin-dependent F-actin organization. Indeed, based on previously reported links between Oskar and F-actin (Krauss et al., 2009; Tanaka et al., 2011), PI4KIIIα may stimulate a

Journal of Cell Science (2014) 127, 954–966 doi:10.1242/jcs.129031

positive feedback loop that coordinates phosphoinositides, actin organization, membrane trafficking and cell polarization.

PI4KIIIα was previously shown to be required in posterior follicle cells (PFCs) to control Hippo signaling, which in turn regulates oocyte nucleus migration and localization of the posterior polarity determinant Staufen (Yan et al., 2011). These defects are similar to those seen in *PI4KIIIα* GLCs. However, our observations suggest that PI4KIIIα probably regulates distinct molecular events in PFCs and the oocyte to control oocyte nucleus migration. In egg chambers with *PI4KIIIα* mutant PFCs, the oocyte nucleus is consistently positioned tightly at the posterior, indicating that mutant PFCs fail to send the unknown signal that initiates oocyte repolarization (Yan et al., 2011). In contrast, the oocyte nucleus in *PI4KIIIα* GLCs is found in the middle of the oocyte, suggesting that a *PI4KIIIα* mutant germline is capable of receiving the unknown signal initiating nucleus migration, but fails to complete the process. Alternatively, tethering of the nucleus to the dorsal-anterior or posterior of the oocyte could be defective in *PI4KIIIα* GLCs. When half of the PFCs are WT and half are mutant for Hippo signaling, normal posterior Staufen and Oskar localization is observed adjacent only to the WT PFCs (Meignin et al., 2007; Polesello and Tapon, 2007; Yu et al., 2008), suggesting that *PI4KIIIα* may be required in both the oocyte and the PFCs for continued communication and maintenance of posterior polarity determinants.

Our study identifies PI4KIIIα as the essential PM PI4K in flies, and shows that it performs a non-overlapping cellular function. Indeed, our results underscore a recurrent theme in phosphoinositide biology: enzymes that nominally act to produce the same lipid can have vastly different physiological and cellular effects. For example, the class II PI3Ks PI3K-C2α and PI3K-C2β both produce PtdIns3*P* and are co-expressed; however, only the latter is necessary for lysophosphatidic-acid-dependent migration of cultured human ovarian and cervical cells (Maffucci et al., 2005). Differential regulation of the enzymes probably results in production of different pools of the same lipid within the cell, emphasizing the importance of identifying factors that control specific pools. Indeed, genetic interactions indicate that Hedgehog relieves Patched inhibition of *Drosophila* PI4KIIIα, suggesting that PI4KIIIα activity is regulated (Yavari et al., 2010). PI4KIIIα also promotes FGF signaling in zebrafish (Ma et al., 2009), Hippo signaling in flies (Yan et al., 2011) and MAPK signaling in yeast (Garrenton et al., 2010). Hence, a crucial and conserved property of this enzyme is to control lipids at the PM, thereby relaying signals to molecular effectors at the cell cortex. Given the multifaceted roles of phosphoinositide signaling in metazoans, it appears that functional diversity of PI4K isoforms has evolved as a mechanism for spatial coordination of phosphoinositide-dependent processes in the cell, with PI4KIIIα acting as a key regulator at the PM.

MATERIALS AND METHODS

Fly stocks and genetic crosses

Flies were raised on standard cornmeal molasses agar at 25℃ (Ashburner, 1990). Visible markers and balancer chromosomes are described by Lindsley and Zimm (Lindsley and Zimm, 1992). Germline transformation of w^{1118} embryos was carried out as in Spradling and Rubin (Spradling and Rubin, 1982). P-element GE3785 was obtained from GenExel (Taejon, Korea). *w;;Δ2–3 Sb/TM2,Ubx* was from Ted Erclik and Howard Lipshitz (University of Toronto, Toronto, ON, Canada). *w*;P{w^+, *UASp::PLCδPH-GFP*} was from Lynn Cooley (Yale University, New Haven, CT) and *w*;P{w^+, *tubP-GAL4*}/*TM3,Sb* was from Eyal Schejter (Weizmann Institute, Rehovot, Israel). *fwd* and *PI4KII* mutants were described previously (Brill et al., 2000; Burgess et al., 2012). Stocks from the Bloomington *Drosophila* Stock Center (Bloomington, IN) were:

l(1)3Ah^{21}*/FM7a/Dp(1;2;Y)w*$^+$
l(1)3Bb^4*/FM7a/Dp(1;2;Y)w*$^+$
sgg^1*/FM7a/Dp(1;2;Y)w*$^+$
P{*FRT(w*^{hs}*)}14A-B*
w ovo^D P{*FRT(w*^{hs}*)}14A-B/C(1)DX/Y;* P{*hsFLP}38*
FM7i, y w B, P{*Act-GFP}JMR3/C(1)DX, y f*

l(1)3Ah^{21} is *zw2*^{c21}, an allele of *zw2*, and *l(1)3Bb*^{4} is an allele of *zw6*.

To generate GLCs by the method of Chou and Perrimon (Chou and Perrimon, 1992), the *PI4KIIIα* deletion was recombined with P{*FRT(w*^{hs}*)}14A-B* and balanced over *FM7i*. GLCs were produced by crossing virgin females to *w ovo*^{D} P{*FRT(w*^{hs}*)}14A-B*/Y; P{*hsFLP}38* males. Females were allowed to lay eggs for 24 hours and emerging larvae were heat-shocked for 2 hours in a 37℃ water bath at 48, 72 and 96 hours. Non-Bar female progeny were aged 7–8 days on yeast paste before dissection.

Generation of the *PI4KIIIα* deletion

To generate a deletion in *PI4KIIIα*, GE3785 (Fig. 1A) was excised imprecisely using Δ2–3 transposase. Deletions were identified by PCR of genomic DNA extracted from 750 candidate flies, pooled into groups of 10. An initial deletion removed the intergenic region between *PI4KIIIα* and the first exon of *sgg*, but left GE3785 intact (GE3785-9). Subsequent mobilization of GE3785-9 removed an additional 1.8 kb from the 3′ end of *PI4KIIIα* (*PI4KIIIα*^{Δ123}).

Neither homozygous *PI4KIIIα*^{Δ123} females nor hemizygous *PI4KIIIα*^{Δ123} males were recovered, indicating *PI4KIIIα* is essential. To determine the lethal period of *PI4KIIIα*^{Δ123} mutants, *PI4KIIIα*^{Δ123}/*FM7i* females were crossed to *FM7i Act-GFP*/Y males. Non-GFP (male) embryos were collected onto agar juice plates and allowed to develop. All embryos hatched, but only *FM7i*/Y larvae reached the adult stage. The others died as L1 larvae, and were presumed to be *PI4KIIIα*^{Δ123}/Y. To assess the ability of the *PI4KIIIα* transgene to rescue viability, *FM7i Act-GFP*/Y males were crossed to *PI4KIIIα*^{Δ123}*;;* P{w^+, *PI4KIIIα*} females. Viable and fertile non-Bar males of genotype *PI4KIIIα*^{Δ123}/Y*;;* P{w^+, *PI4KIIIα*}/+ were recovered in equal numbers to female siblings.

Molecular biology

The *PI4KIIIα* rescue transgene was generated as a genomic–cDNA fusion. The 5′ half, consisting of genomic DNA encoding *PI4KIIIα*, was joined to the 3′ half, containing cDNA (EST clone SD12145; Canadian *Drosophila* Microarray Centre, Mississauga, Ontario, Canada). Genomic DNA containing the 5′ rescuing region was amplified from w^{1118} flies using primers 5′-GCTCTAGAGCTTCGATATTTTCCGCTTTTTAGC-3′ and 5′-ATCTGCTGCACACCCTGGTA-3′, and cloned into pBluescript with *Xba*I and *Kpn*I. cDNA subcloned from SD12145 as a *Kpn*I–*Mlu*I fragment was ligated with a *Mlu*I–*Xma*I PCR product containing the 3′UTR from SD12145, amplified using 5′-AACT-TCCGCACGCGTACCTAC-3′ and 5′-CCCCCCGGGGGGCGTTAGA-ACGCGGCTACAAT-3′, into pBluescript with *Kpn*I and *Xma*I. Genomic and cDNA fragments were fused at a unique internal *Kpn*I site and cloned into pBluescript with *Xba*I and *Xma*I. The genomic–cDNA construct was subcloned into pCaSpeR4 using *Xba*I and the blunt-cutters *Sma*I and *Stu*I.

PI4KIIIα, *fwd*, *PI4KII* and *sktl* double-stranded RNA (dsRNA) templates were prepared by PCR amplification of genomic DNA from w^{1118} flies. *slik* dsRNA was amplified from EST LD34405. As a negative control, *GFP* dsRNA was amplified from the pEGFP-N2 plasmid. Oligonucleotides included (top strand) a 5′ T3 promoter sequence (5′-AATTAACCCTCACTAAAGGGAGA-3′) or (bottom strand) a 5′ T7 promoter sequence (5′-TTAATACGACTCACTATAGGGAGA-3′). Gene-specific sequences were: *PI4KIIIα* exon 5 (5′-GAGTGCCACA-AATCCAACCT-3′ and 5′-ACGAACAGTTCCAGCAGCTT-3′); *PI4KIIIα* exon 6 start (5′-CGATCAGTACCTCTCCTTTC-3′ and 5′-CCTTATCC-TTCTCGCTAAGTA-3′); *PI4KIIIα* exon 6 end (5′-TGAAGTTCTGGC-AGACGATG-3′ and 5′-CGGCAGACTATTGGGATTGT-3′); *fwd* (5′-CC-AAGAATGCCATATTTCGC-3′ and 5′-GGAGCACATCAGACACAGG-

3′); *PI4KII* (5′-TTCGTGGAGGGTTACAAGG-3′ and 5′-AAGGGAAAA-GCGAGACCAT-3′); *sktl* exon 1 start (5′-GCAGCAGGAACTGAAC-AACA-3′ and 5′-CGTAGACCTTGAAGCGGAAG-3′); *sktl* exon 1 middle (5′-GGTTGGTGGCCATGAACAA-3′ and 5′-ACGCTGACGATTCATA-CTG-3′); *slik* (5′-CTCCAGTCACCACGGCTATTG-3′ and 5′-CGACG-GAGGAGCAGGAACCAC-3′); *GFP* (5′-GACGTAAACGGCCACAAG-TT-3′ and 5′-TGTTCTGCTGGTAGTGGTCG-3′). dsRNA was prepared using MegaScript T7 and T3 *in vitro* transcription kits (Ambion, Applied Biosystems, Carlsbad, CA). Equal amounts of the T3 and T7 transcription products were mixed, heated to 95℃ for 10 minutes and cooled slowly to room temperature to anneal. Double knockdown of *fwd* and *PI4KII* was verified by qRT-PCR (supplementary material Fig. S1).

Cell culture and dsRNA treatment

S2 cell culture, dsRNA treatments, cell lysis and immunoblotting were performed essentially as described previously (Hipfner et al., 2004). Blots were probed with rabbit anti-phospho-Ezrin/Radixin/Moesin (no. 3141; Cell Signaling Technology Inc., Danvers, MA) and then re-probed with rabbit anti-*Drosophila* Moe [a gift from Daniel Kiehart (Duke University, Durham, NC)]. Signals in immunoblots were quantified using the 'Gel' function of ImageJ 1.42q. Moe phosphorylation levels were expressed as the ratio of phosphorylated to total Moe signals, and were normalized to the ratio observed in *GFP*-dsRNA-treated cells. Statistical analysis for comparison of pMoe levels in *PI4KIIIα* versus *fwd* and *PI4KII* knockdown experiments was performed with results from triplicate dsRNA treatments.

Quantification of mRNA knockdown in dsRNA experiments

Drosophila S2 cells adapted to growth in serum-free medium (EX-CELL 420; Sigma) supplemented with 16.5 nM L-glutamine and 1× penicillin–streptomycin (Invitrogen) were plated in 24-well plates in 1 ml medium containing a total of 8 µg dsRNA. For single knockdowns, 4 µg of *slik* or *PI4KIIIα* dsRNA plus 4 µg of control (*lacZ*) dsRNA were used. For double knockdown, 4 µg of *PI4KII* plus 4 µg of *fwd* dsRNA were used. For the control sample, 8 µg of *lacZ* dsRNA were used. Five days later, cells were rinsed once with PBS and total RNA extracted using TRIzol (Life Technologies) according to manufacturer's instructions. cDNA was prepared using the High Capacity cDNA Reverse Transcription Kit (Invitrogen). qPCR reactions were set up with SYBR Select Master Mix (Life Technologies) and run on a ViiA 7 Real-Time PCR System (Life Technologies). Gene-specific primers used for amplification were: *fwd*, 5′-TGACGCCGATCATCTCTTGTCCAT-3′ and 5′-TTCTCGGTGCG-ACTATGTGCTCAA-3′; *PI4KII*, 5′-TCTTCAGCTTGGCCTTCTGTC-GAT-3′ and 5′-TTAAGCCAAAGGACGAGGAACCCT-3′; *PI4KIIIα*, 5′-AGTCCCTCCAGGCAAACC-3′ and 5′-AGCTGCAGAATAAACA-GCAGGA-3′; *slik*, 5′-CCTGCATCGCAACAAAGTCATCCA-3′ and 5′-AGTAGGGAGTGCCAATGAAGGTGT-3′; *rpl32* (for normalization), 5′-AAGAAGCGCACCAAGCACTTCATC-3′ and 5′-ACGCACTCTGT-TGTCGATACCCTT-3′. The effect of RNAi on Moe phosphorylation and on localization of a Golgi PtdIns4*P* marker was verified (not shown).

Immunocytochemistry

Immunolocalization was performed using standard procedures (Máthé, 2004). Ovaries were fixed in buffer B fixative (3:2:1 solution of distilled H_2O:16% paraformaldehyde:buffer B) for 15 minutes. Buffer B consists of 100 mM KH_2PO_4/K_2HPO_4 pH 6.8, 450 mM KCl, 150 mM NaCl, 20 mM $MgCl_2$. Rhodamine–phalloidin was used at 4 U/ml, dried and resuspended in ethanol before addition (Invitrogen Corp., Carlsbad, CA). ToPro DNA dye was used at 1:1000 (Invitrogen) and samples were mounted in PPD (0.1× PBS, 90% glycerol, 1 mg/ml *p*-phenylenediamine). Immunolocalization of phosphatidylinositol phosphates was performed as described previously (Hammond et al., 2009).

The following antibodies were used: rabbit anti-Oskar (a gift from Paul Lasko, McGill University; 1:700), rabbit anti-phospho-Moe (Cell Signaling; 1:700), mouse anti-Sec5 22A2 (DSHB; 1:200) (Murthy et al., 2003), mouse anti-Gurken 1D12 (DSHB; 1:300) (Queenan et al., 1999), mouse anti-FasIII 7G10 (DSHB; 1:50) (Patel et al., 1987), rabbit anti-Lva (a gift from John Sisson, University of Texas at Austin; 1:2000), mouse anti-phosphatidylinositol phosphate IgM antibodies (Echelon Biosciences Inc., Salt Lake City, UT) were used at 1:100 (anti-PtdIns4*P*) or 1:400 [anti-PtdIns(4,5)P_2]. Fluorescein- or Texas-Red-labeled *Lycopersicon esculentum* (tomato) lectin (Vector Laboratories Inc., Burlingame, CA) was used at 150 µg/ml. Anti-rabbit and anti-mouse IgG or IgM secondary antibodies conjugated to Alexa Fluor 488 or 568 (Molecular Probes, Invitrogen, Carlsbad, CA) were used at 1:1000.

Imaging and analysis

Images were acquired on either a Zeiss Axiovert 100 inverted laser scanning confocal microscope using LSM510 software or on a Zeiss Axioplan 2 upright fluorescence microscope with a Zeiss Axiocam CCD camera using Axiovision 4.8 software (Oberkochen, Baden-Württemberg, Germany). Images of phosphatidylinositol phosphate staining were acquired with a Nikon Eclipse Ti inverted scanning confocal microscope using NIS Elements AR software (Melville, NY). When necessary, images used for comparison were adjusted for levels, brightness and contrast in an identical manner using Adobe Photoshop CS5. Staging of WT egg chambers was performed according to Spradling (Spradling, 1993). Mutant GLCs were staged on the basis of the most prominent developmental hallmark(s). The oocyte nucleus position was scored in WT and *PI4KIIIα* GLCs judged to be stage 8 or later by vitellogenesis, size and shape of the oocyte relative to the egg chamber, and follicle cell morphology.

Ovaries were prepared for transmission electron microscopy as described previously (Bazinet and Rollins, 2003). Images were obtained using AmtV542 acquisition software (Advanced Microscopy Techniques, Woburn, MA, USA).

Lva and lectin puncta size was measured using Volocity 4. Puncta within one plane of a representative egg chamber were scored using the line measurement tool across the greatest cross-sectional distance for each spot. Statistical analysis was performed using one-way and two-way ANOVA followed by Tukey's pairwise comparison post-test. Sec5, PtdIns4*P*, PtdIns(4,5)P_2 and F-actin intensity levels of representative egg chambers were quantified using ImageJ 1.43u. Statistical analysis of phosphatidylinositol phosphate:F-actin intensity ratios between WT and *PI4KIIIα* was performed with the paired Student's *t*-test using average intensities normalized to WT.

Acknowledgements

We thank members of the Brill and Hipfner labs and Trudi Schupbach for helpful discussions; Lauren Del Bel and Jonathan Ma for technical assistance; Dorothea Godt and Paul Lasko for valuable comments on the manuscript; Lynn Cooley, Eyal Schejter, Paul Lasko, Dan Kiehart, Ted Erclik, Howard Lipshitz, John Sisson, the Developmental Studies Hybridoma Bank, the Bloomington *Drosophila* Stock Center and GenExel for generously providing flies and reagents; Michael Woodside and Paul Paroutis (SickKids Imaging Facility) for assistance with confocal imaging; and Janet Rollins, Doug Holmyard and Yew Meng Heng for assistance with transmission electron microscopy.

Competing interests

The authors declare no competing interests.

Author contributions

J.T. designed, performed and analyzed all experiments except dsRNA experiments and co-wrote the manuscript; K.O. performed dsRNA experiments; J.B. designed the screen for the *PI4KIIIα* mutant and edited the manuscript; D.R.H. designed and analyzed the dsRNA experiments and edited the manuscript; J.A.B. conceived and designed the project and co-wrote the manuscript.

Funding

This work was supported by SickKids Restracomp [to J.T.]; the Canadian Institutes of Health Research [grant numbers MOP #81187 and #106426 to D.R.H.]; the University of Toronto Connaught Fund [to J.A.B.]; and The Cancer Research Society, Inc. [to J.A.B.].

Supplementary material

Supplementary material available online at
http://jcs.biologists.org/lookup/suppl/doi:10.1242/jcs.129031/-/DC1

References

Ashburner, M. (1990). *Drosophila: A Laboratory Handbook*. Cold Spring Harbor, NY: Cold Spring Harbor Press.

Audhya, A. and Emr, S. D. (2002). Stt4 PI 4-kinase localizes to the plasma membrane and functions in the Pkc1-mediated MAP kinase cascade. *Dev. Cell* **2**, 593-605.

Audhya, A., Foti, M. and Emr, S. D. (2000). Distinct roles for the yeast phosphatidylinositol 4-kinases, Stt4p and Pik1p, in secretion, cell growth, and organelle membrane dynamics. *Mol. Biol. Cell* **11**, 2673-2689.

Balla, A. and Balla, T. (2006). Phosphatidylinositol 4-kinases: old enzymes with emerging functions. *Trends Cell Biol.* **16**, 351-361.

Balla, A., Tuymetova, G., Tsiomenko, A., Várnai, P. and Balla, T. (2005). A plasma membrane pool of phosphatidylinositol 4-phosphate is generated by phosphatidylinositol 4-kinase type-III alpha: studies with the PH domains of the oxysterol binding protein and FAPP1. *Mol. Biol. Cell* **16**, 1282-1295.

Bazinet, C. and Rollins, J. E. (2003). Rickettsia-like mitochondrial motility in Drosophila spermiogenesis. *Evol. Dev.* **5**, 379-385.

Beronja, S., Laprise, P., Papoulas, O., Pellikka, M., Sisson, J. and Tepass, U. (2005). Essential function of Drosophila Sec6 in apical exocytosis of epithelial photoreceptor cells. *J. Cell Biol.* **169**, 635-646.

Bogard, N., Lan, L., Xu, J. and Cohen, R. S. (2007). Rab11 maintains connections between germline stem cells and niche cells in the Drosophila ovary. *Development* **134**, 3413-3418.

Brill, J. A., Hime, G. R., Scharer-Schuksz, M. and Fuller, M. T. (2000). A phospholipid kinase regulates actin organization and intercellular bridge formation during germline cytokinesis. *Development* **127**, 3855-3864.

Brill, J. A., Wong, R. and Wilde, A. (2011). Phosphoinositide function in cytokinesis. *Curr. Biol.* **21**, R930-R934.

Burgess, J., Del Bel, L. M., Ma, C. I., Barylko, B., Polevoy, G., Rollins, J., Albanesi, J. P., Krämer, H. and Brill, J. A. (2012). Type II phosphatidylinositol 4-kinase regulates trafficking of secretory granule proteins in Drosophila. *Development* **139**, 3040-3050.

Chou, T. B. and Perrimon, N. (1992). Use of a yeast site-specific recombinase to produce female germline chimeras in Drosophila. *Genetics* **131**, 643-653.

Coutelis, J. B. and Ephrussi, A. (2007). Rab6 mediates membrane organization and determinant localization during Drosophila oogenesis. *Development* **134**, 1419-1430.

D'Angelo, G., Vicinanza, M., Wilson, C. and De Matteis, M. A. (2012). Phosphoinositides in Golgi complex function. *Subcell. Biochem.* **59**, 255-270.

Dollar, G., Struckhoff, E., Michaud, J. and Cohen, R. S. (2002). Rab11 polarization of the Drosophila oocyte: a novel link between membrane trafficking, microtubule organization, and oskar mRNA localization and translation. *Development* **129**, 517-526.

Echard, A. (2012). Phosphoinositides and cytokinesis: the "PIP" of the iceberg. *Cytoskeleton (Hoboken)* **69**, 893-912.

Fabian, L., Wei, H. C., Rollins, J., Noguchi, T., Blankenship, J. T., Bellamkonda, K., Polevoy, G., Gervais, L., Guichet, A., Fuller, M. T. et al. (2010). Phosphatidylinositol 4,5-bisphosphate directs spermatid cell polarity and exocyst localization in Drosophila. *Mol. Biol. Cell* **21**, 1546-1555.

Fievet, B. T., Gautreau, A., Roy, C., Del Maestro, L., Mangeat, P., Louvard, D. and Arpin, M. (2004). Phosphoinositide binding and phosphorylation act sequentially in the activation mechanism of ezrin. *J. Cell Biol.* **164**, 653-659.

Gaidarov, I. and Keen, J. H. (1999). Phosphoinositide-AP-2 interactions required for targeting to plasma membrane clathrin-coated pits. *J. Cell Biol.* **146**, 755-764.

Garrenton, L. S., Stefan, C. J., McMurray, M. A., Emr, S. D. and Thorner, J. (2010). Pheromone-induced anisotropy in yeast plasma membrane phosphatidylinositol-4,5-bisphosphate distribution is required for MAPK signaling. *Proc. Natl. Acad. Sci. USA* **107**, 11805-11810.

Gervais, L., Claret, S., Januschke, J., Roth, S. and Guichet, A. (2008). PIP5K-dependent production of PIP2 sustains microtubule organization to establish polarized transport in the Drosophila oocyte. *Development* **135**, 3829-3838.

Hammond, G. R., Schiavo, G. and Irvine, R. F. (2009). Immunocytochemical techniques reveal multiple, distinct cellular pools of PtdIns4P and PtdIns(4,5)P(2). *Biochem. J.* **422**, 23-35.

Hammond, G. R., Fischer, M. J., Anderson, K. E., Holdich, J., Koteci, A., Balla, T. and Irvine, R. F. (2012). PI4P and PI(4,5)P2 are essential but independent lipid determinants of membrane identity. *Science* **337**, 727-730.

Han, G. S., Audhya, A., Markley, D. J., Emr, S. D. and Carman, G. M. (2002). The Saccharomyces cerevisiae LSB6 gene encodes phosphatidylinositol 4-kinase activity. *J. Biol. Chem.* **277**, 47709-47718.

He, B., Xi, F., Zhang, X., Zhang, J. and Guo, W. (2007). Exo70 interacts with phospholipids and mediates the targeting of the exocyst to the plasma membrane. *EMBO J.* **26**, 4053-4065.

Hipfner, D. R., Keller, N. and Cohen, S. M. (2004). Slik Sterile-20 kinase regulates Moesin activity to promote epithelial integrity during tissue growth. *Genes Dev.* **18**, 2243-2248.

Jankovics, F., Sinka, R., Lukácsovich, T. and Erdélyi, M. (2002). MOESIN crosslinks actin and cell membrane in Drosophila oocytes and is required for OSKAR anchoring. *Curr. Biol.* **12**, 2060-2065.

Januschke, J., Nicolas, E., Compagnon, J., Formstecher, E., Goud, B. and Guichet, A. (2007). Rab6 and the secretory pathway affect oocyte polarity in Drosophila. *Development* **134**, 3419-3425.

Jović, M., Kean, M. J., Szentpetery, Z., Polevoy, G., Gingras, A. C., Brill, J. A. and Balla, T. (2012). Two phosphatidylinositol 4-kinases control lysosomal delivery of the Gaucher disease enzyme, β-glucocerebrosidase. *Mol. Biol. Cell* **23**, 1533-1545.

Judd, B. H., Shen, M. W. and Kaufman, T. C. (1972). The anatomy and function of a segment of the X chromosome of Drosophila melanogaster. *Genetics* **71**, 139-156.

Khuong, T. M., Habets, R. L., Slabbaert, J. R. and Verstreken, P. (2010). WASP is activated by phosphatidylinositol-4,5-bisphosphate to restrict synapse growth in a pathway parallel to bone morphogenetic protein signaling. *Proc. Natl. Acad. Sci. USA* **107**, 17379-17384.

Krauss, J., López de Quinto, S., Nüsslein-Volhard, C. and Ephrussi, A. (2009). Myosin-V regulates oskar mRNA localization in the Drosophila oocyte. *Curr. Biol.* **19**, 1058-1063.

Langevin, J., Morgan, M. J., Sibarita, J. B., Aresta, S., Murthy, M., Schwarz, T., Camonis, J. and Bellaïche, Y. (2005). Drosophila exocyst components Sec5, Sec6, and Sec15 regulate DE-Cadherin trafficking from recycling endosomes to the plasma membrane. *Dev. Cell* **9**, 365-376.

Lindsley, D. L. and Zimm, G. G. (1992). *The Genome of Drosophila Melanogaster*. San Diego, CA: Academic Press.

Ma, H., Blake, T., Chitnis, A., Liu, P. and Balla, T. (2009). Crucial role of phosphatidylinositol 4-kinase IIIalpha in development of zebrafish pectoral fin is linked to phosphoinositide 3-kinase and FGF signaling. *J. Cell Sci.* **122**, 4303-4310.

Maffucci, T., Cooke, F. T., Foster, F. M., Traer, C. J., Fry, M. J. and Falasca, M. (2005). Class II phosphoinositide 3-kinase defines a novel signaling pathway in cell migration. *J. Cell Biol.* **169**, 789-799.

Martin, T. F. (2012). Role of PI(4,5)P(2) in vesicle exocytosis and membrane fusion. *Subcell. Biochem.* **59**, 111-130.

Marygold, S. J., Leyland, P. C., Seal, R. L., Goodman, J. L., Thurmond, J., Strelets, V. B., Wilson, R. J.; FlyBase consortium (2013). FlyBase: improvements to the bibliography. *Nucleic Acids Res.* **41**, D751-D757.

Máthé, E. (2004). Immunocytological analysis of oogenesis. *Methods Mol. Biol.* **247**, 89-127.

Meignin, C., Alvarez-Garcia, I., Davis, I. and Palacios, I. M. (2007). The salvador-warts-hippo pathway is required for epithelial proliferation and axis specification in Drosophila. *Curr. Biol.* **17**, 1871-1878.

Murphy, A. M. and Montell, D. J. (1996). Cell type-specific roles for Cdc42, Rac, and RhoL in Drosophila oogenesis. *J. Cell Biol.* **133**, 617-630.

Murray, M. J., Ng, M. M., Fraval, H., Tan, J., Liu, W., Smallhorn, M., Brill, J. A., Field, S. J. and Saint, R. (2012). Regulation of Drosophila mesoderm migration by phosphoinositides and the PH domain of the Rho GTP exchange factor Pebble. *Dev. Biol.* **372**, 17-27.

Murthy, M. and Schwarz, T. L. (2004). The exocyst component Sec5 is required for membrane traffic and polarity in the Drosophila ovary. *Development* **131**, 377-388.

Murthy, M., Garza, D., Scheller, R. H. and Schwarz, T. L. (2003). Mutations in the exocyst component Sec5 disrupt neuronal membrane traffic, but neurotransmitter release persists. *Neuron* **37**, 433-447.

Murthy, M., Ranjan, R., Denef, N., Higashi, M. E., Schupbach, T. and Schwarz, T. L. (2005). Sec6 mutations and the Drosophila exocyst complex. *J. Cell Sci.* **118**, 1139-1150.

Nakatsu, F., Baskin, J. M., Chung, J., Tanner, L. B., Shui, G., Lee, S. Y., Pirruccello, M., Hao, M., Ingolia, N. T., Wenk, M. R. et al. (2012). PtdIns4P synthesis by PI4KIIIα at the plasma membrane and its impact on plasma membrane identity. *J. Cell Biol.* **199**, 1003-1016.

Patel, N. H., Snow, P. M. and Goodman, C. S. (1987). Characterization and cloning of fasciclin III: a glycoprotein expressed on a subset of neurons and axon pathways in Drosophila. *Cell* **48**, 975-988.

Perrimon, N., Engstrom, L. and Mahowald, A. P. (1989). Zygotic lethals with specific maternal effect phenotypes in Drosophila melanogaster. I. Loci on the X chromosome. *Genetics* **121**, 333-352.

Polesello, C. and Tapon, N. (2007). Salvador-warts-hippo signaling promotes Drosophila posterior follicle cell maturation downstream of notch. *Curr. Biol.* **17**, 1864-1870.

Polesello, C., Delon, I., Valenti, P., Ferrer, P. and Payre, F. (2002). Dmoesin controls actin-based cell shape and polarity during Drosophila melanogaster oogenesis. *Nat. Cell Biol.* **4**, 782-789.

Polevoy, G., Wei, H. C., Wong, R., Szentpetery, Z., Kim, Y. J., Goldbach, P., Steinbach, S. K., Balla, T. and Brill, J. A. (2009). Dual roles for the Drosophila PI 4-kinase four wheel drive in localizing Rab11 during cytokinesis. *J. Cell Biol.* **187**, 847-858.

Queenan, A. M., Barcelo, G., Van Buskirk, C. and Schüpbach, T. (1999). The transmembrane region of Gurken is not required for biological activity, but is necessary for transport to the oocyte membrane in Drosophila. *Mech. Dev.* **89**, 35-42.

Raghu, P., Coessens, E., Manifava, M., Georgiev, P., Pettitt, T., Wood, E., Garcia-Murillas, I., Okkenhaug, H., Trivedi, D., Zhang, Q. et al. (2009). Rhabdomere biogenesis in Drosophila photoreceptors is acutely sensitive to phosphatidic acid levels. *J. Cell Biol.* **185**, 129-145.

Raucher, D., Stauffer, T., Chen, W., Shen, K., Guo, S., York, J. D., Sheetz, M. P. and Meyer, T. (2000). Phosphatidylinositol 4,5-bisphosphate functions as a second messenger that regulates cytoskeleton-plasma membrane adhesion. *Cell* **100**, 221-228.

Roch, F., Polesello, C., Roubinet, C., Martin, M., Roy, C., Valenti, P., Carreno, S., Mangeat, P. and Payre, F. (2010). Differential roles of PtdIns(4,5)P2 and phosphorylation in moesin activation during Drosophila development. *J. Cell Sci.* **123**, 2058-2067.

Roth, S., Neuman-Silberberg, F. S., Barcelo, G. and Schüpbach, T. (1995). cornichon and the EGF receptor signaling process are necessary for both anterior-posterior and dorsal-ventral pattern formation in Drosophila. *Cell* **81**, 967-978.

Roubinet, C., Decelle, B., Chicanne, G., Dorn, J. F., Payrastre, B., Payre, F. and Carreno, S. (2011). Molecular networks linked by Moesin drive remodeling of the cell cortex during mitosis. *J. Cell Biol.* **195**, 99-112.

Saarikangas, J., Zhao, H. and Lappalainen, P. (2010). Regulation of the actin cytoskeleton-plasma membrane interplay by phosphoinositides. *Physiol. Rev.* **90**, 259-289.

Shannon, M. P., Kaufman, T. C., Shen, M. W. and Judd, B. H. (1972). Lethality patterns and morphology of selected lethal and semi-lethal mutations in the zeste-white region of Drosophila melanogaster. *Genetics* **72**, 615-638.

Shewan, A., Eastburn, D. J. and Mostov, K. (2011). Phosphoinositides in cell architecture. *Cold Spring Harb. Perspect. Biol.* **3**, a004796.

Simons, J. P., Al-Shawi, R., Minogue, S., Waugh, M. G., Wiedemann, C., Evangelou, S., Loesch, A., Sihra, T. S., King, R., Warner, T. T. et al. (2009). Loss of phosphatidylinositol 4-kinase 2alpha activity causes late onset degeneration of spinal cord axons. *Proc. Natl. Acad. Sci. USA* **106**, 11535-11539.

Spradling, A. C. (1993). Developmental genetics of oogenesis. In *The Development of Drosophila Melanogaster*, Vol. 1 (ed. M. Bate and A. Martinez Arias), pp. 1-70. Cold Spring Harbor, NY: Cold Spring Harbor Laboratory Press.

Spradling, A. C. and Rubin, G. M. (1982). Transposition of cloned P elements into Drosophila germ line chromosomes. *Science* **218**, 341-347.

Strahl, T., Hama, H., DeWald, D. B. and Thorner, J. (2005). Yeast phosphatidylinositol 4-kinase, Pik1, has essential roles at the Golgi and in the nucleus. *J. Cell Biol.* **171**, 967-979.

Tanaka, T., Kato, Y., Matsuda, K., Hanyu-Nakamura, K. and Nakamura, A. (2011). Drosophila Mon2 couples Oskar-induced endocytosis with actin remodeling for cortical anchorage of the germ plasm. *Development* **138**, 2523-2532.

Thapa, N., Sun, Y., Schramp, M., Choi, S., Ling, K. and Anderson, R. A. (2012). Phosphoinositide signaling regulates the exocyst complex and polarized integrin trafficking in directionally migrating cells. *Dev. Cell* **22**, 116-130.

Vallis, Y., Wigge, P., Marks, B., Evans, P. R. and McMahon, H. T. (1999). Importance of the pleckstrin homology domain of dynamin in clathrin-mediated endocytosis. *Curr. Biol.* **9**, 257-263.

Verdier, V., Johndrow, J. E., Betson, M., Chen, G. C., Hughes, D. A., Parkhurst, S. M. and Settleman, J. (2006). Drosophila Rho-kinase (DRok) is required for tissue morphogenesis in diverse compartments of the egg chamber during oogenesis. *Dev. Biol.* **297**, 417-432.

von Stein, W., Ramrath, A., Grimm, A., Müller-Borg, M. and Wodarz, A. (2005). Direct association of Bazooka/PAR-3 with the lipid phosphatase PTEN reveals a link between the PAR/aPKC complex and phosphoinositide signaling. *Development* **132**, 1675-1686.

Weixel, K. M., Blumental-Perry, A., Watkins, S. C., Aridor, M. and Weisz, O. A. (2005). Distinct Golgi populations of phosphatidylinositol 4-phosphate regulated by phosphatidylinositol 4-kinases. *J. Biol. Chem.* **280**, 10501-10508.

Wu, S., Mehta, S. Q., Pichaud, F., Bellen, H. J. and Quiocho, F. A. (2005). Sec15 interacts with Rab11 via a novel domain and affects Rab11 localization in vivo. *Nat. Struct. Mol. Biol.* **12**, 879-885.

Xiong, X., Xu, Q., Huang, Y., Singh, R. D., Anderson, R., Leof, E., Hu, J. and Ling, K. (2012). An association between type Iγ PI4P 5-kinase and Exo70 directs E-cadherin clustering and epithelial polarization. *Mol. Biol. Cell* **23**, 87-98.

Yan, Y., Denef, N., Tang, C. and Schüpbach, T. (2011). Drosophila PI4KIIIalpha is required in follicle cells for oocyte polarization and Hippo signaling. *Development* **138**, 1697-1703.

Yavari, A., Nagaraj, R., Owusu-Ansah, E., Folick, A., Ngo, K., Hillman, T., Call, G., Rohatgi, R., Scott, M. P. and Banerjee, U. (2010). Role of lipid metabolism in smoothened derepression in hedgehog signaling. *Dev. Cell* **19**, 54-65.

Yu, J., Poulton, J., Huang, Y. C. and Deng, W. M. (2008). The hippo pathway promotes Notch signaling in regulation of cell differentiation, proliferation, and oocyte polarity. *PloS One* **3**, e1761.

Zhang, L., Mao, Y. S., Janmey, P. A. and Yin, H. L. (2012). Phosphatidylinositol 4, 5 bisphosphate and the actin cytoskeleton. *Subcell. Biochem.* **59**, 177-215.